

A visualization of the cosmic web, showing a complex network of dark matter filaments and galaxy clusters. The filaments are depicted as thin, blue, thread-like structures, while the clusters are represented by dense, orange and yellow regions. The background is a deep blue, suggesting the vastness of space.

Baryons and non-Gaussian statistics for weak lensing cosmology

Daniela Grandón
Leiden University

In collab with Elena Sellentin, Jia Liu, Gabriela Marques, Sihao Cheng, Joaquin Armijo++

arXiv:2308.10866, 2403.03807

Grandón & Sellentin in prep. 2024

COSMO21, 21 May 2024, Chania 

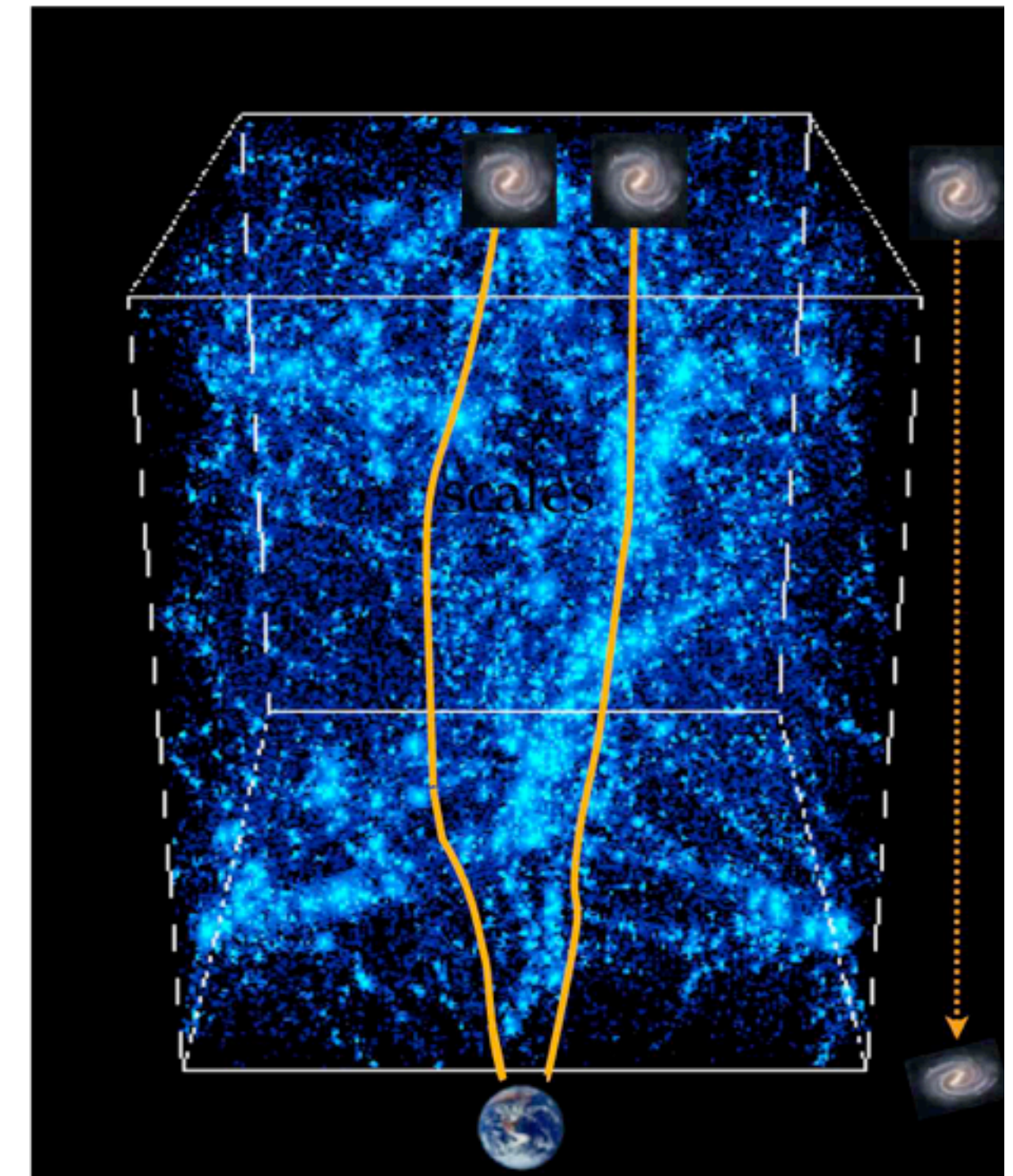
A visualization of the cosmic web, showing a complex network of dark matter filaments and clusters of galaxies. The filaments are depicted as thin, blue, thread-like structures, while the galaxy clusters are shown as dense, orange and yellow regions. The background is a deep, dark blue, suggesting the vastness of the universe.

Weak lensing cosmology and non-Gaussian fields

Weak gravitational lensing: convergence

Weak lensing convergence (κ) maps are 2D projections of the matter density along the line of sight.

$$\kappa(\boldsymbol{\theta}) = \frac{3H_0^2\Omega_m}{2c^2} \int_0^{\chi_{lim}} d\chi g(\chi) \chi \frac{\delta(\chi\boldsymbol{\theta}, \chi)}{a(\chi)}$$

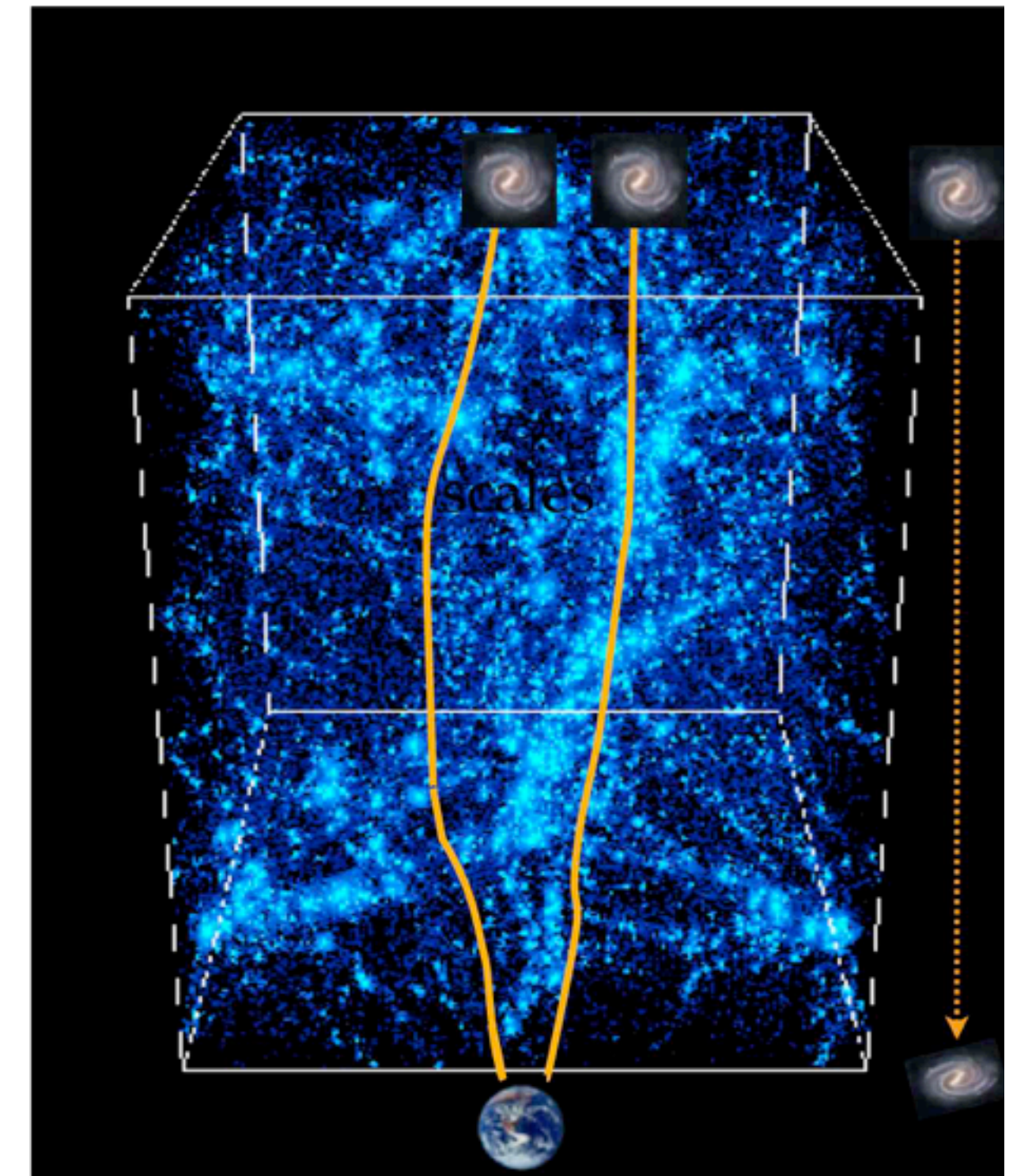


Weak gravitational lensing: convergence

Weak lensing convergence (κ) maps are 2D projections of the matter density along the line of sight.

$$\kappa(\boldsymbol{\theta}) = \frac{3H_0^2\Omega_m}{2c^2} \int_0^{\chi_{lim}} d\chi g(\chi) \chi \frac{\delta(\chi\boldsymbol{\theta}, \chi)}{a(\chi)}$$

$$g(\chi) = \int_{\chi}^{\chi_s} d\chi' n(\chi') \frac{\chi' - \chi}{\chi}$$



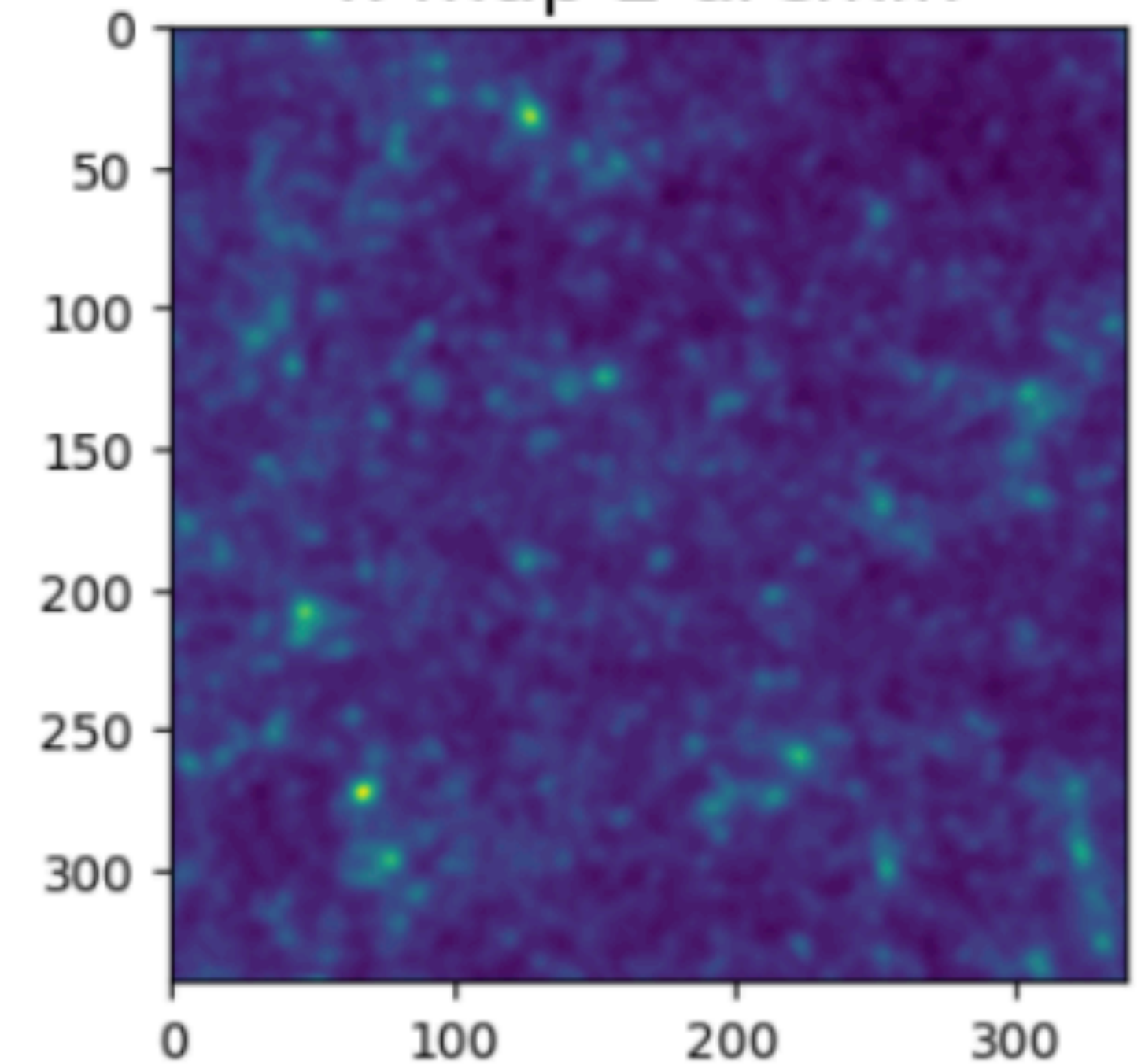
Weak gravitational lensing: convergence

Weak lensing convergence (κ) maps are 2D projections of the matter density along the line of sight.

$$\kappa(\boldsymbol{\theta}) = \frac{3H_0^2\Omega_m}{2c^2} \int_0^{\chi_{lim}} d\chi g(\chi) \chi \frac{\delta(\chi\boldsymbol{\theta}, \chi)}{a(\chi)}$$

$$g(\chi) = \int_{\chi}^{\chi_s} d\chi' n(\chi') \frac{\chi' - \chi}{\chi}$$

Convergence map
 κ -map 2 arcmin



Weak gravitational lensing: convergence

Weak lensing convergence (κ) maps are 2D projections of the matter density along the line of sight.

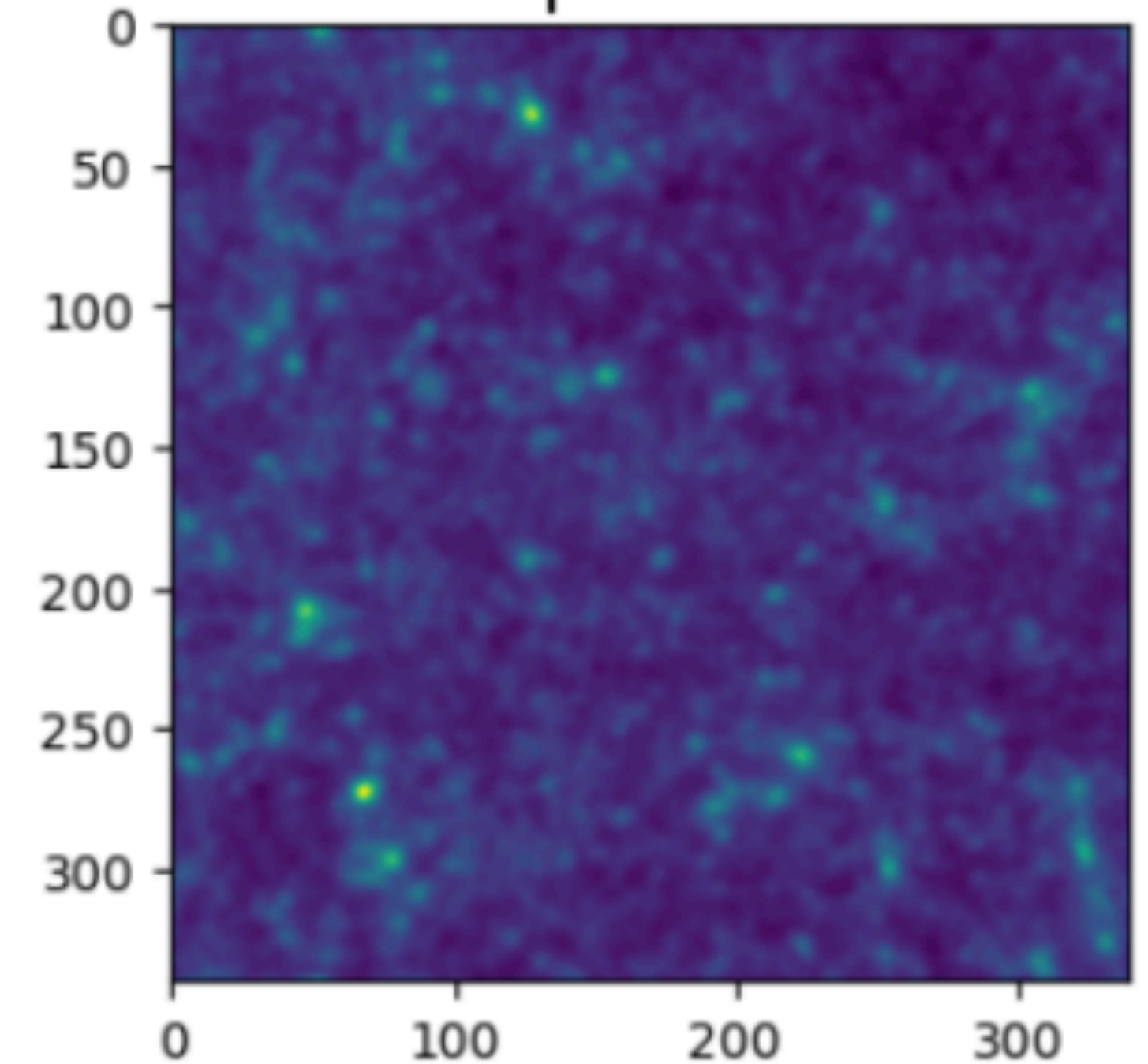
$$\kappa(\boldsymbol{\theta}) = \frac{3H_0^2\Omega_m}{2c^2} \int_0^{\chi_{lim}} d\chi g(\chi) \chi \frac{\delta(\chi\boldsymbol{\theta}, \chi)}{a(\chi)}$$

$$g(\chi) = \int_{\chi}^{\chi_s} d\chi' n(\chi') \frac{\chi' - \chi}{\chi}$$

Convergence power spectrum

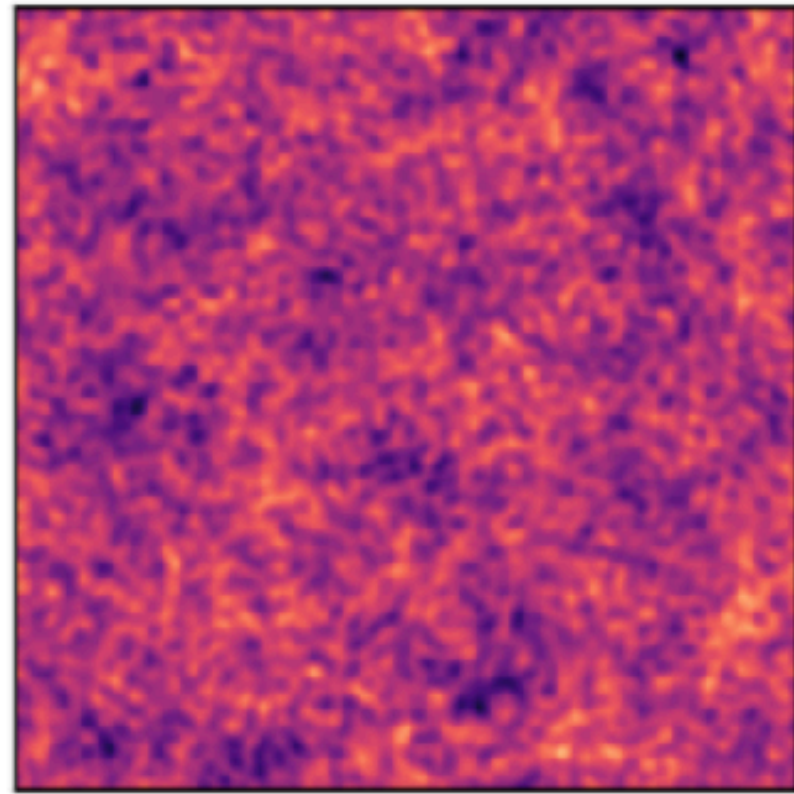
$$C_{\kappa}(\ell) = \frac{9H_0^4\Omega_m}{4c^4} \int_0^{\chi_s} d\chi \frac{g^2(\chi)\chi}{a^2(\chi)} P_{\delta} \left(k = \frac{\ell}{\chi}, \chi \right)$$

Convergence map
 κ -map 2 arcmin

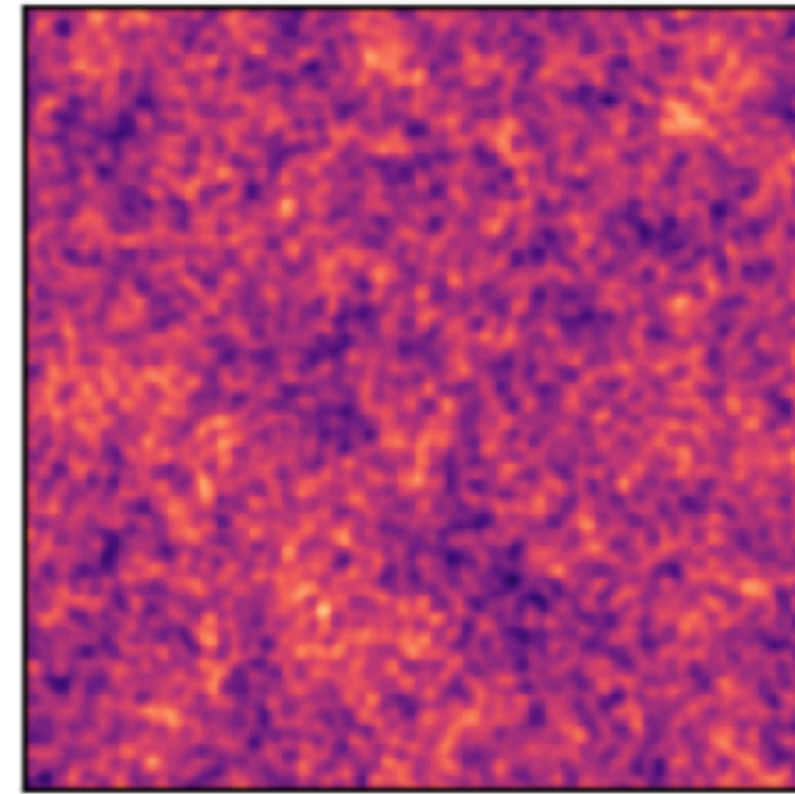


Extracting non-Gaussian information

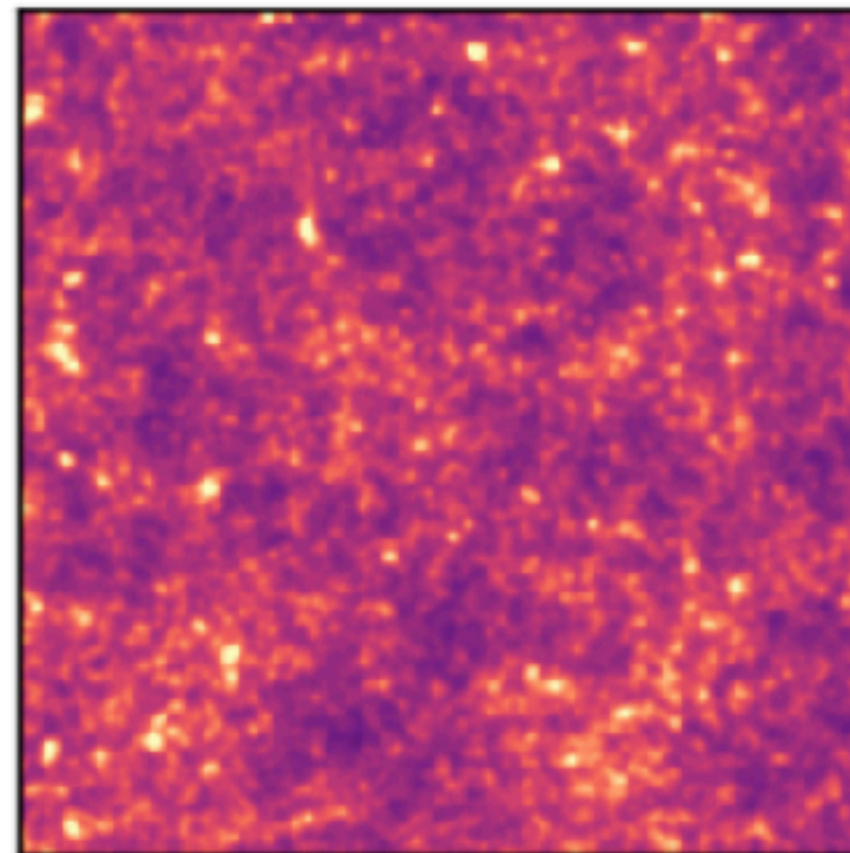
Map 1



Map 2

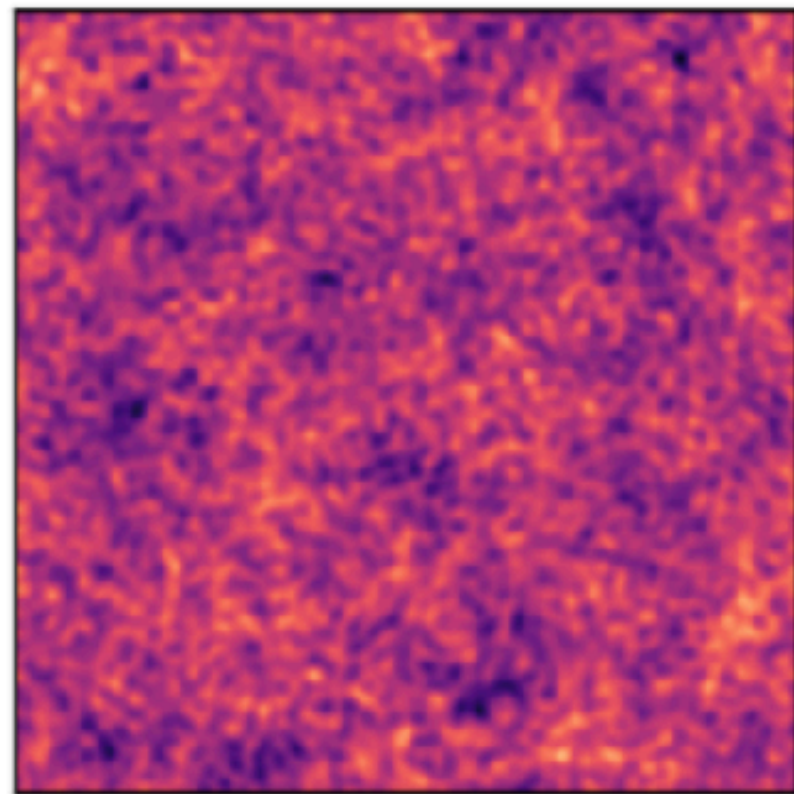


Map 3

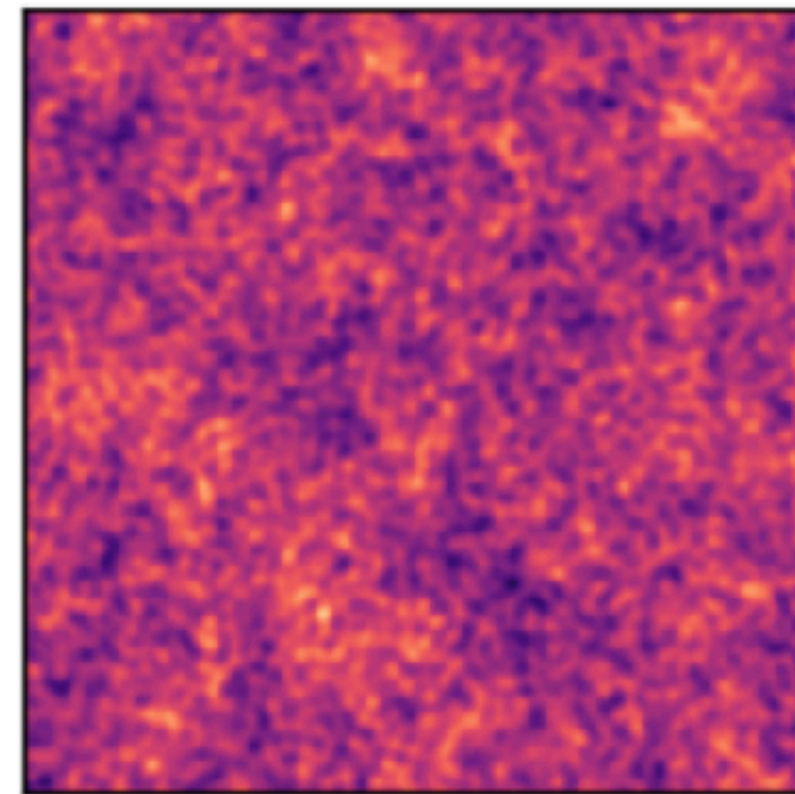


Extracting non-Gaussian information

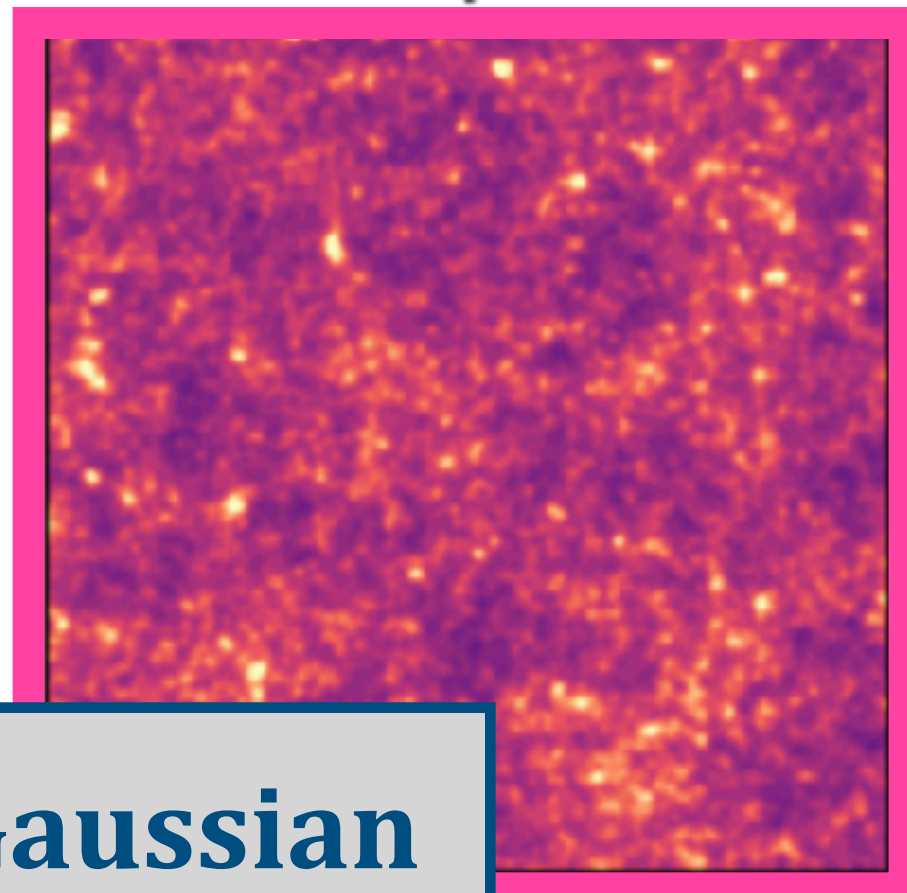
Map 1



Map 2

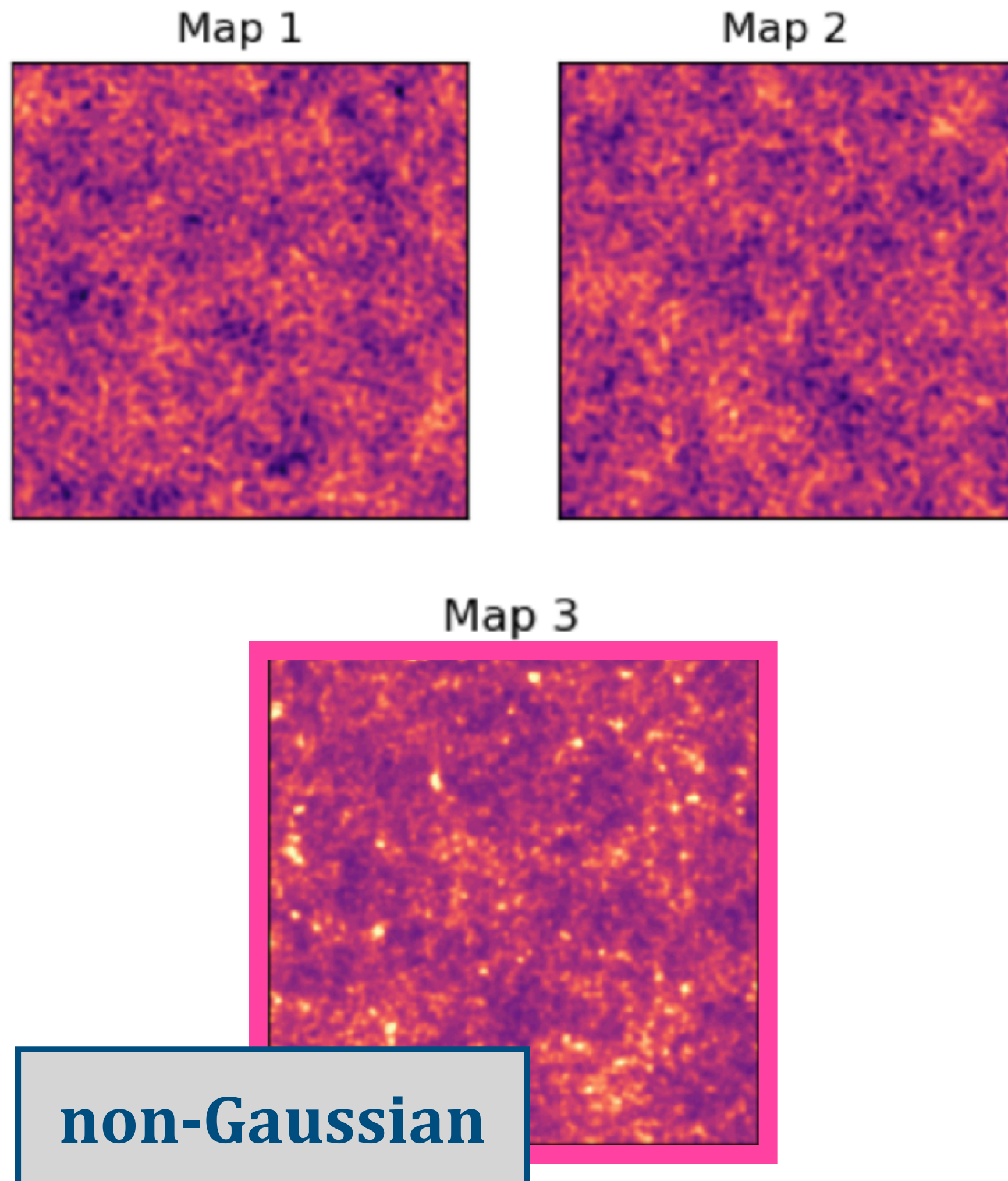


Map 3

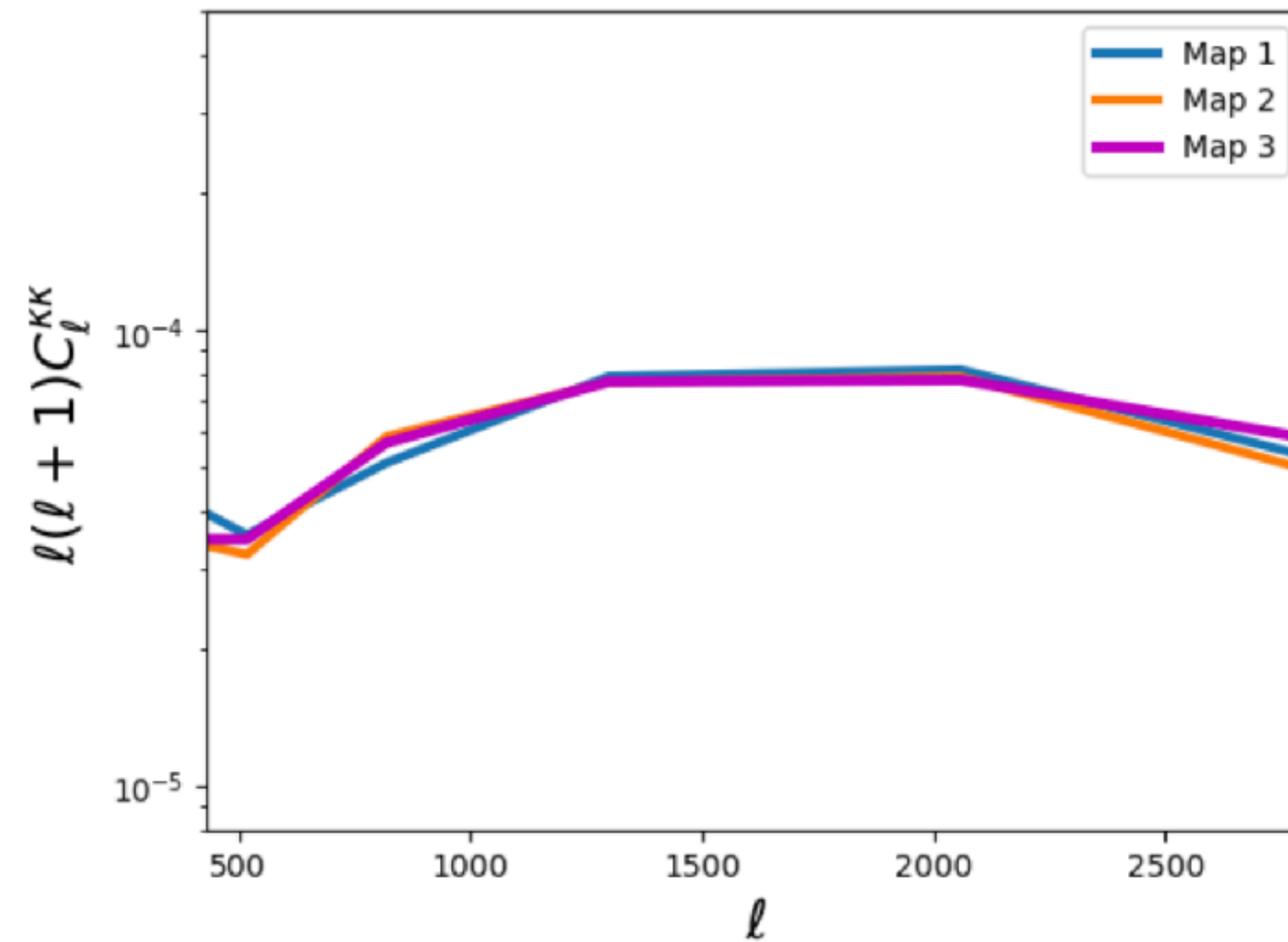


non-Gaussian

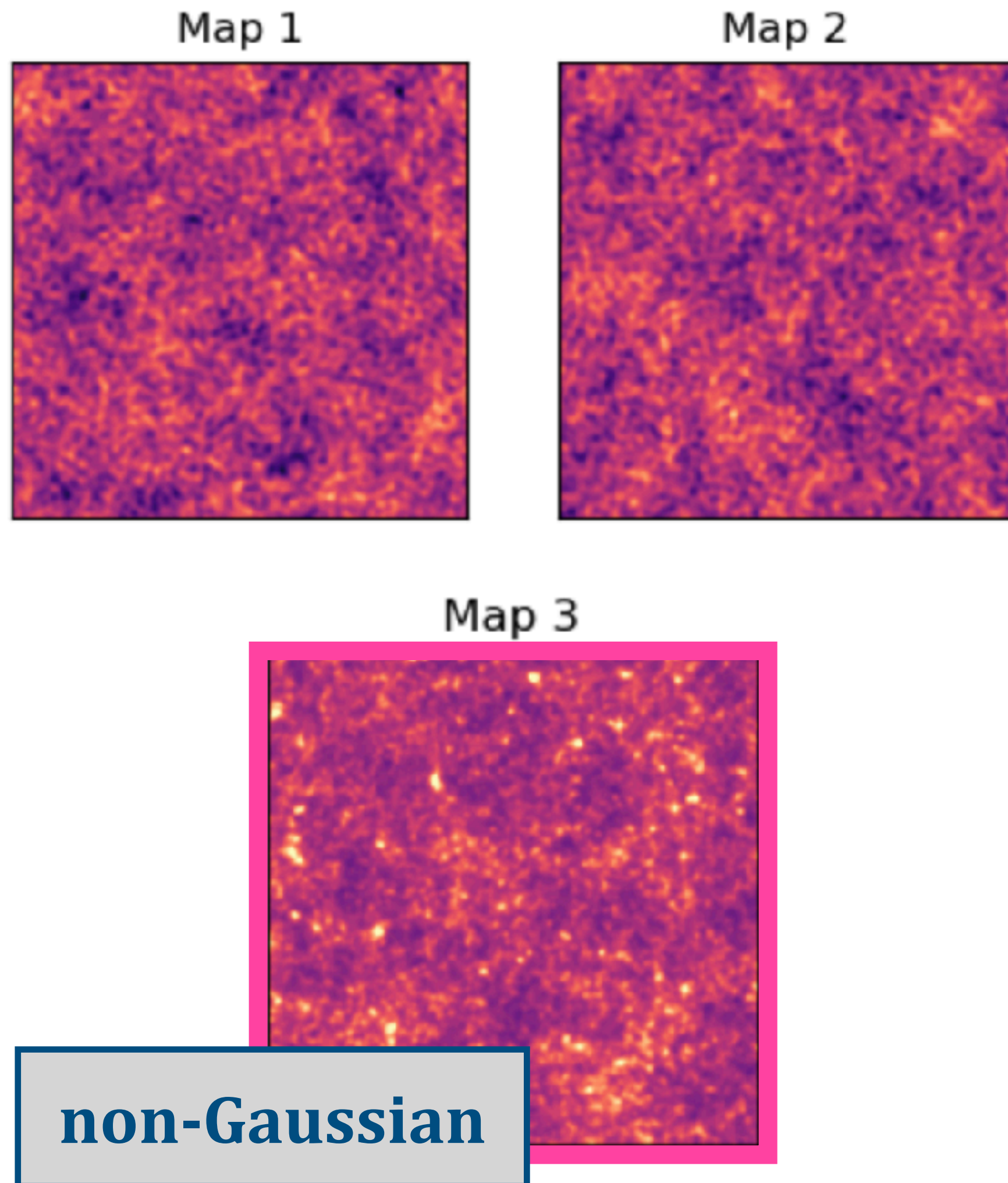
Extracting non-Gaussian information



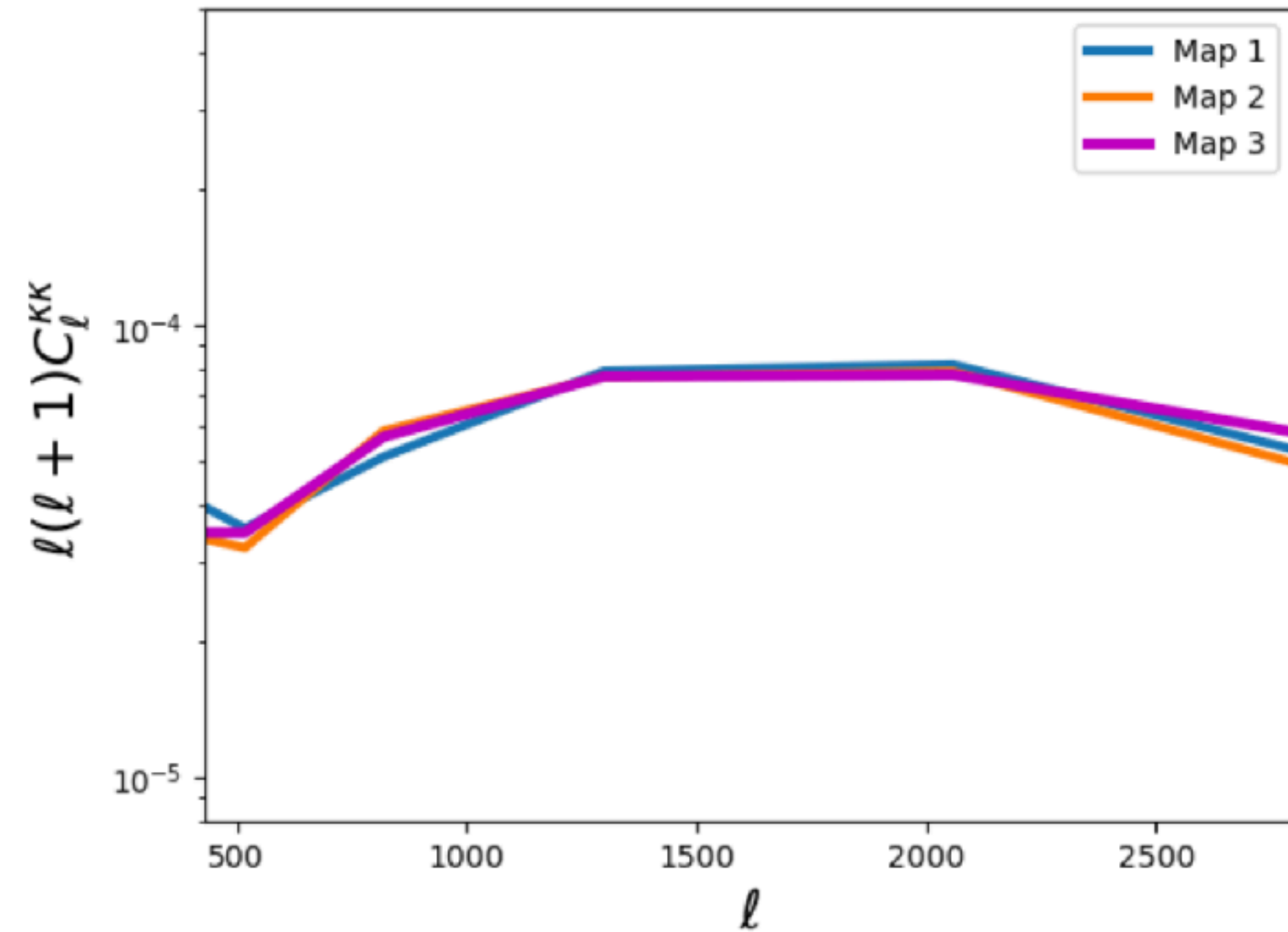
Same power spectrum



Extracting non-Gaussian information



Same power spectrum



We need to go beyond 2point information!

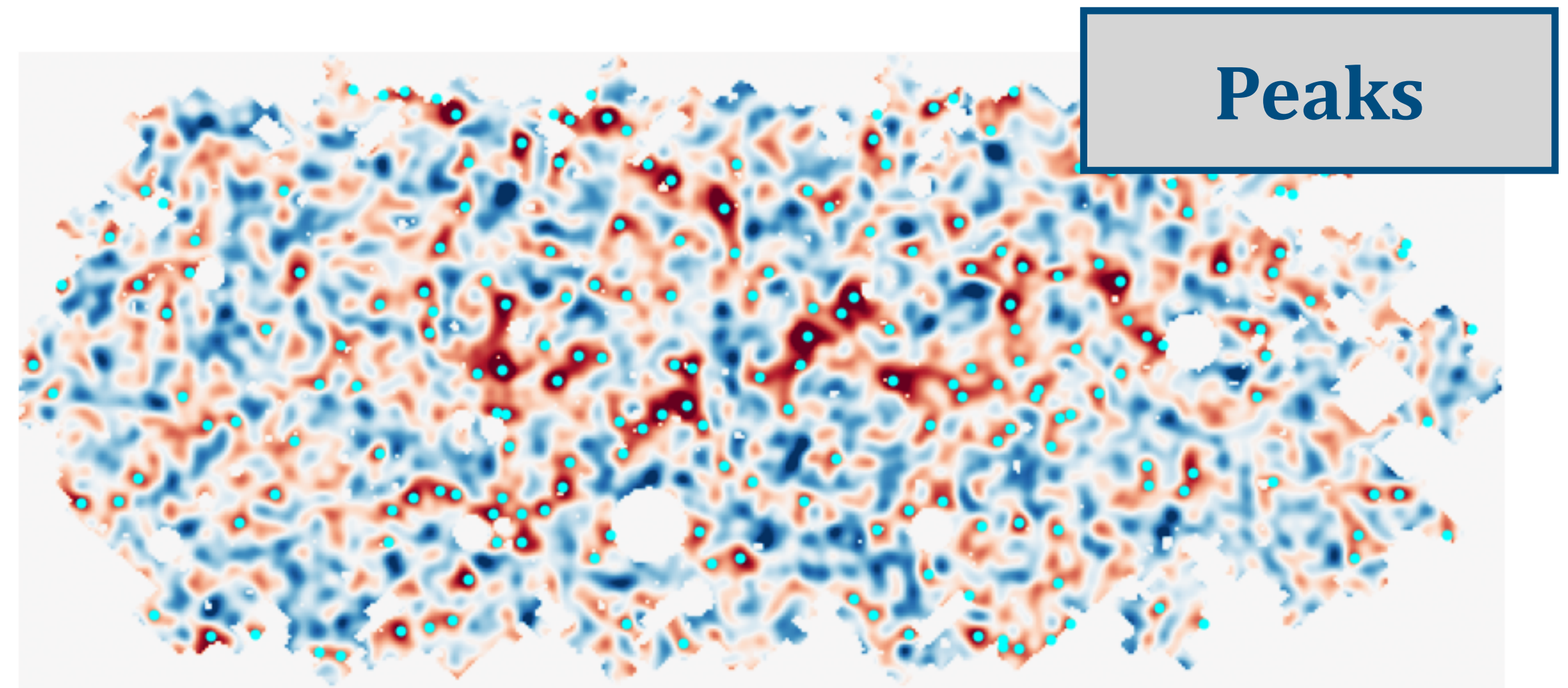
➔ Non-Gaussian, higher order statistics

A visualization of the cosmic web, showing a complex network of dark matter filaments and galaxy clusters. The filaments are depicted as thin, blue, fibrous structures, while the clusters are represented by dense, orange and yellow regions. The overall structure is highly non-Gaussian and hierarchical.

Non-Gaussian, higher-order statistics

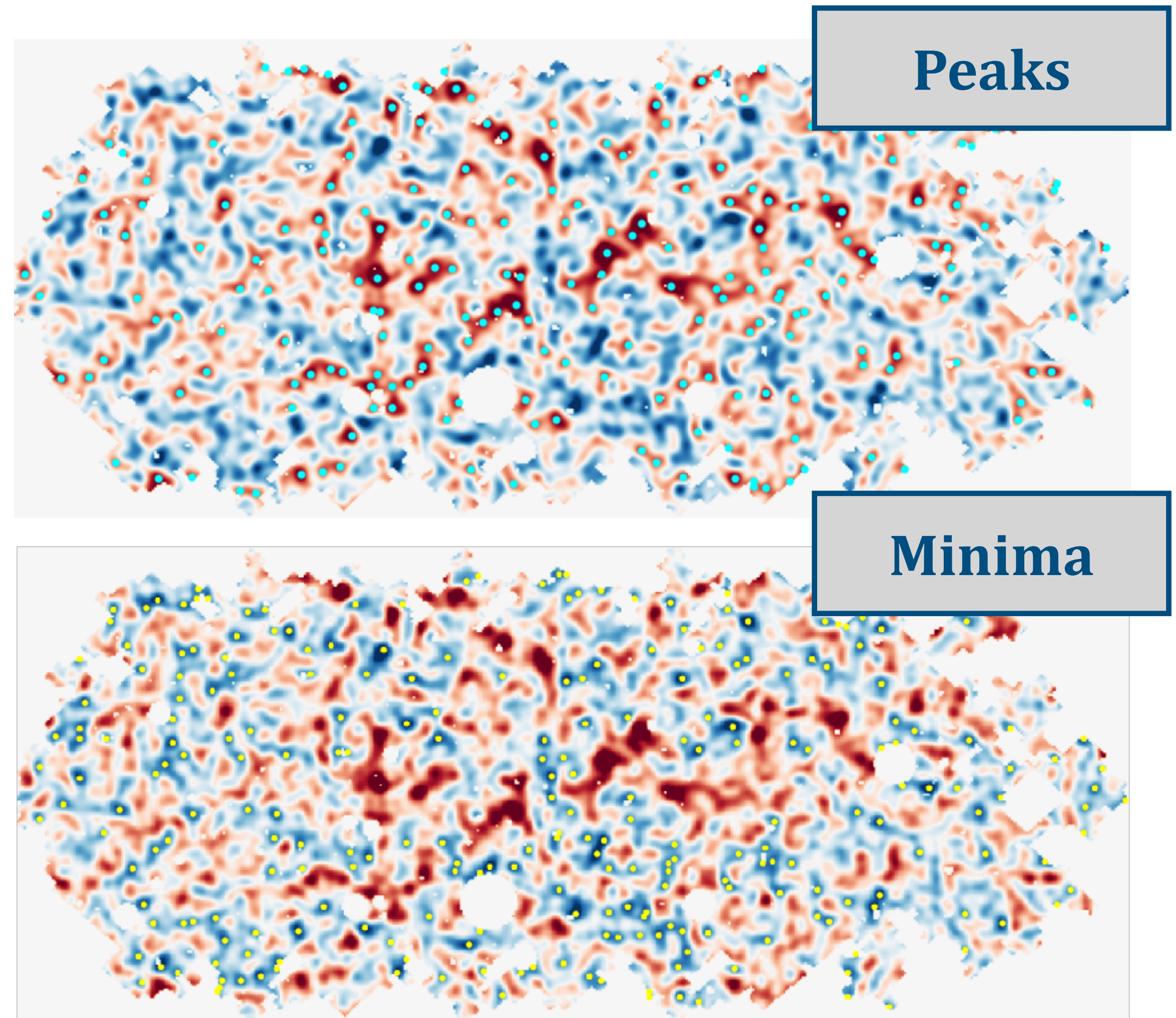
Non-Gaussian statistics

- **Peak counts:**
Probe overdense regions, massive clusters along the line of sight.



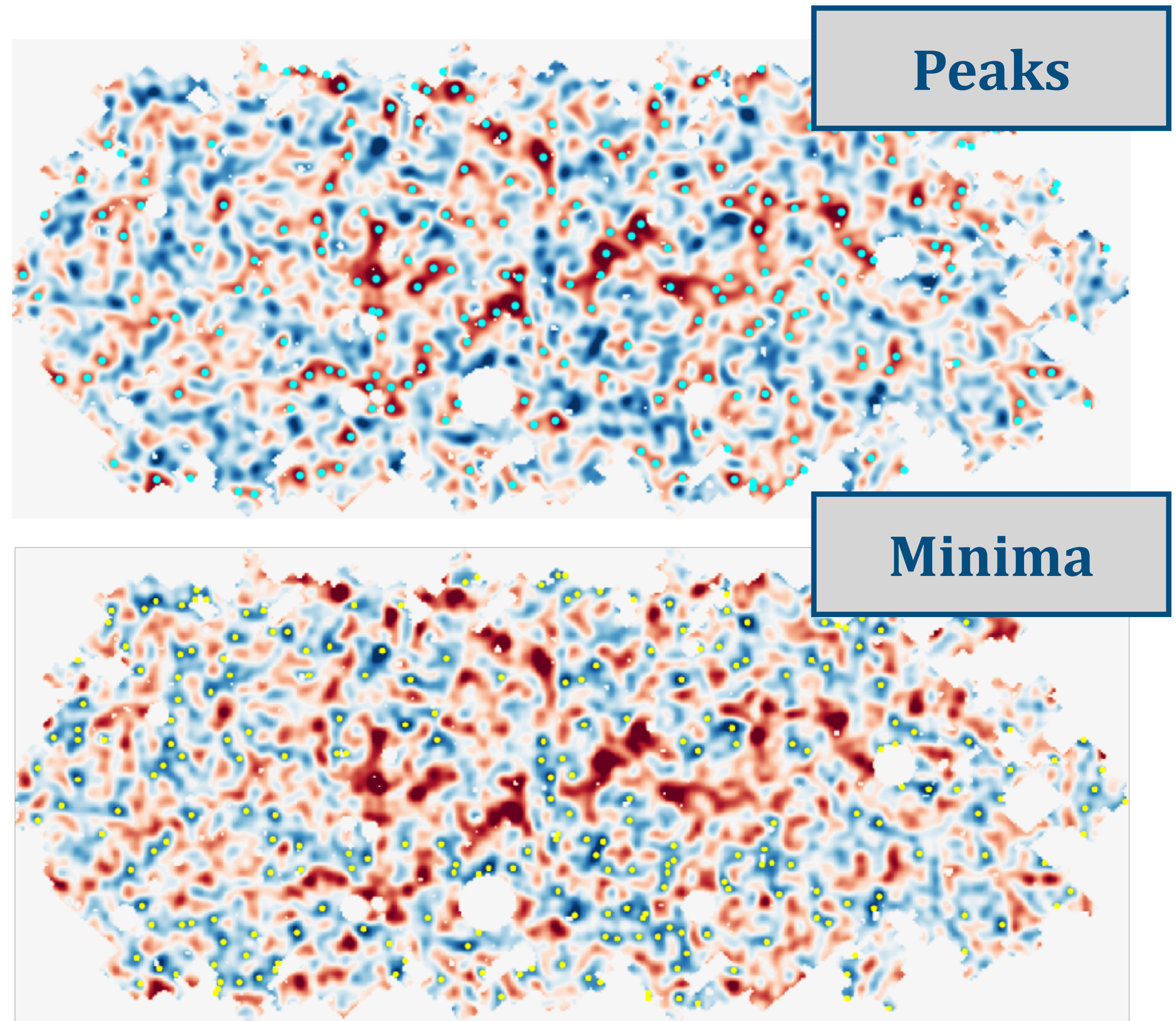
Non-Gaussian statistics

- **Peak counts:**
Probe overdense regions, massive clusters along the line of sight.
- **Minimum counts:** Probe the emptiest/underdense regions.



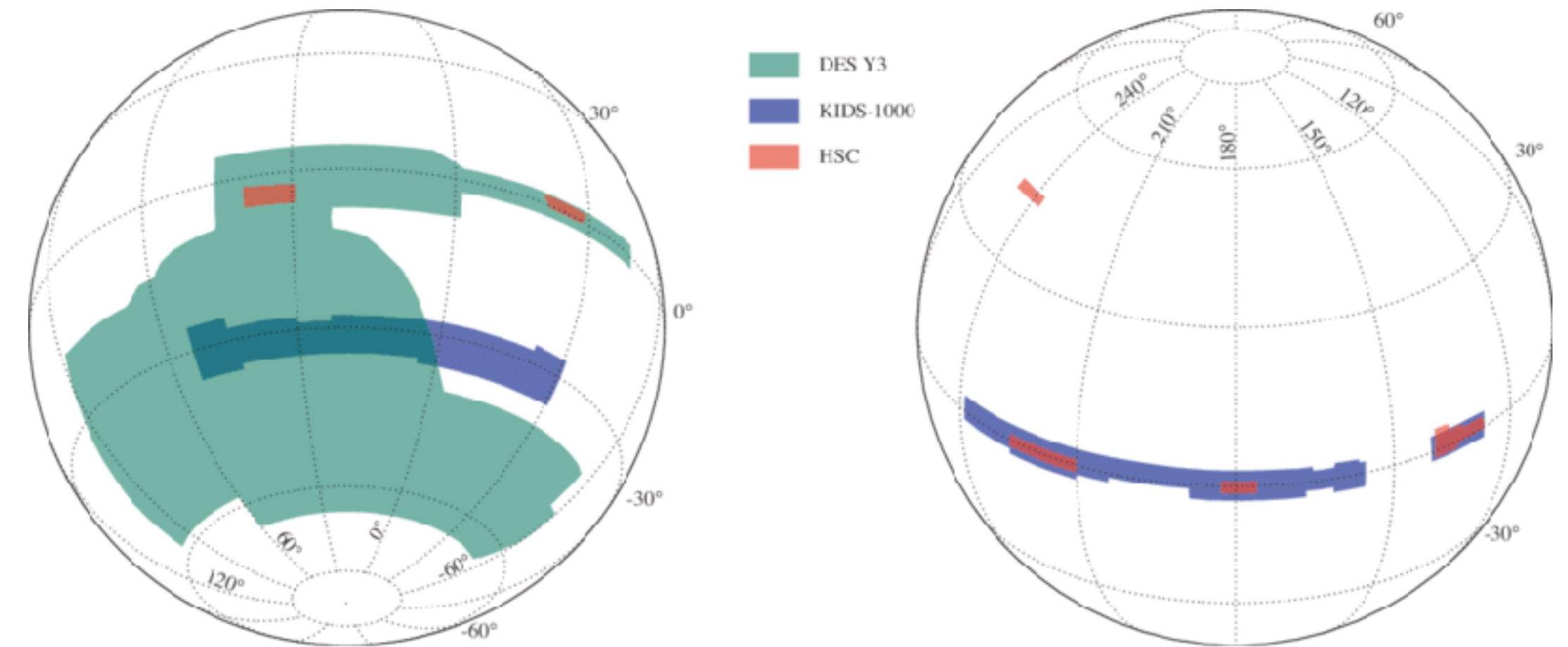
Non-Gaussian statistics

- **Peak counts:**
Probe overdense regions, massive clusters along the line of sight.
- **Minimum counts:** Probe the emptiest/underdense regions.
- **PDF:** Histogram of convergence values.



Stage III analysis: Subaru Hyper Suprime-Cam Y1 data

- ➔ Y1 data: 137 deg^2
- ➔ $n_{\text{gal}} = 17 \text{ arcmin}^{-2}$
- ➔ Likelihood based on N-body sims
- ➔ **Model the statistics with emulators.**

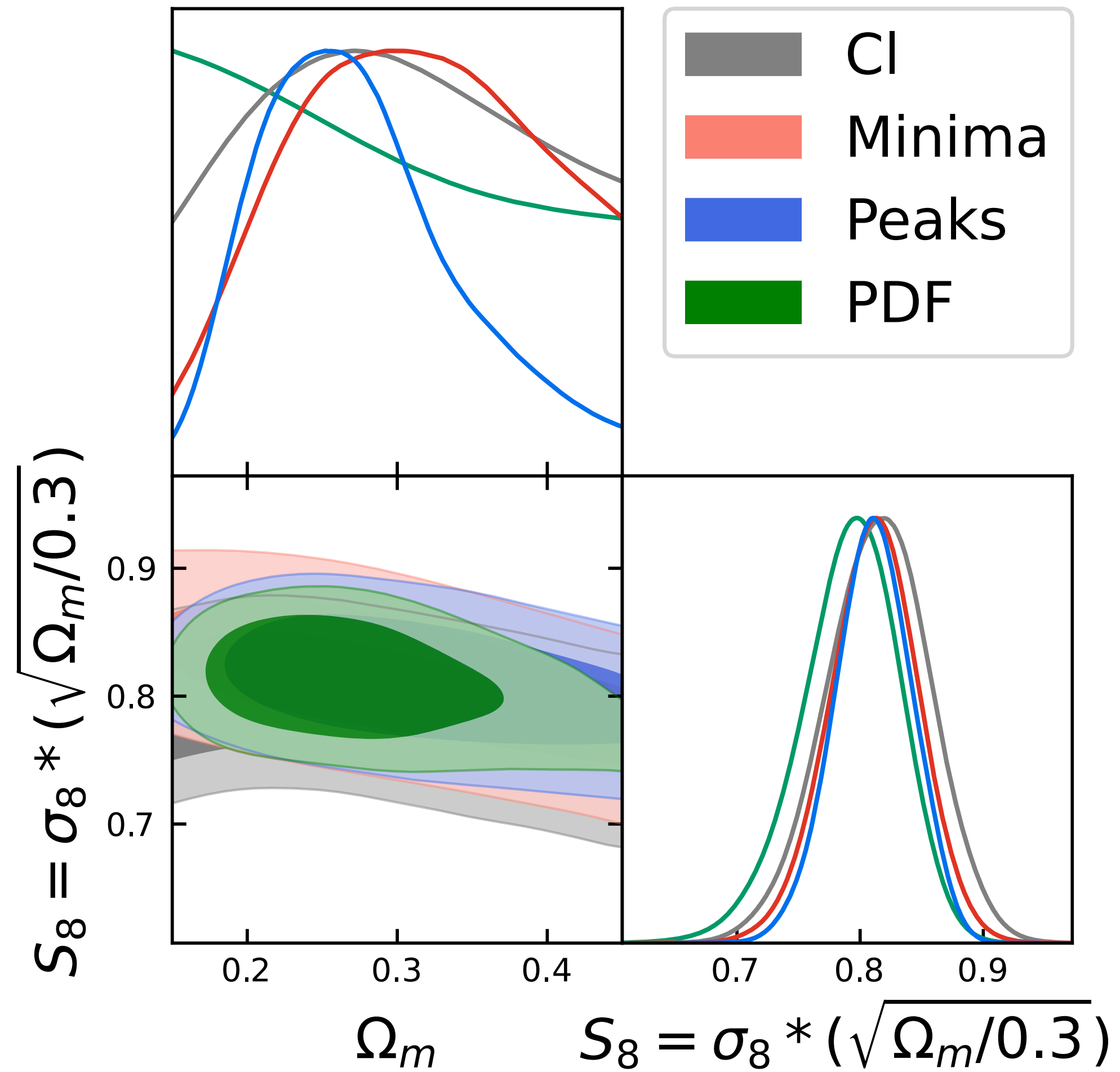


z -range	$n_g^{\text{eff}} [\text{arcmin}^{-2}]$
$0.3 < z < 0.6$	5.14
$0.6 < z < 0.9$	5.23
$0.9 < z < 1.2$	3.99
$1.2 < z < 1.5$	2.33

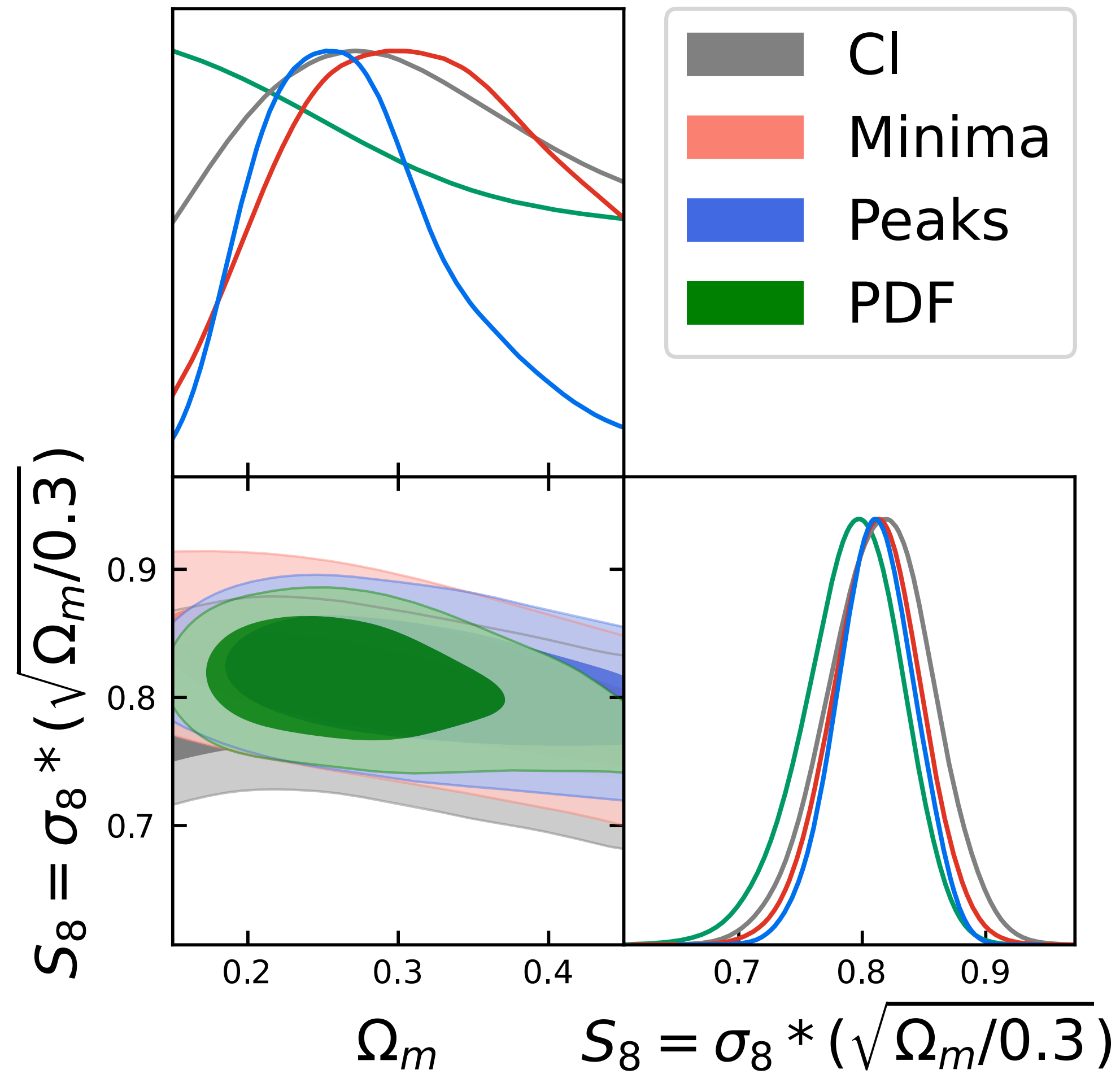
Marques et al. 2023, Grandón et al. 2024

Thiele et al. 2023, Cheng et al. 2024, Armijo et al. in prep 2024

Results Stage III: HSC Y1 Non-Gaussian statistics



Results Stage III: HSC Y1 Non-Gaussian statistics



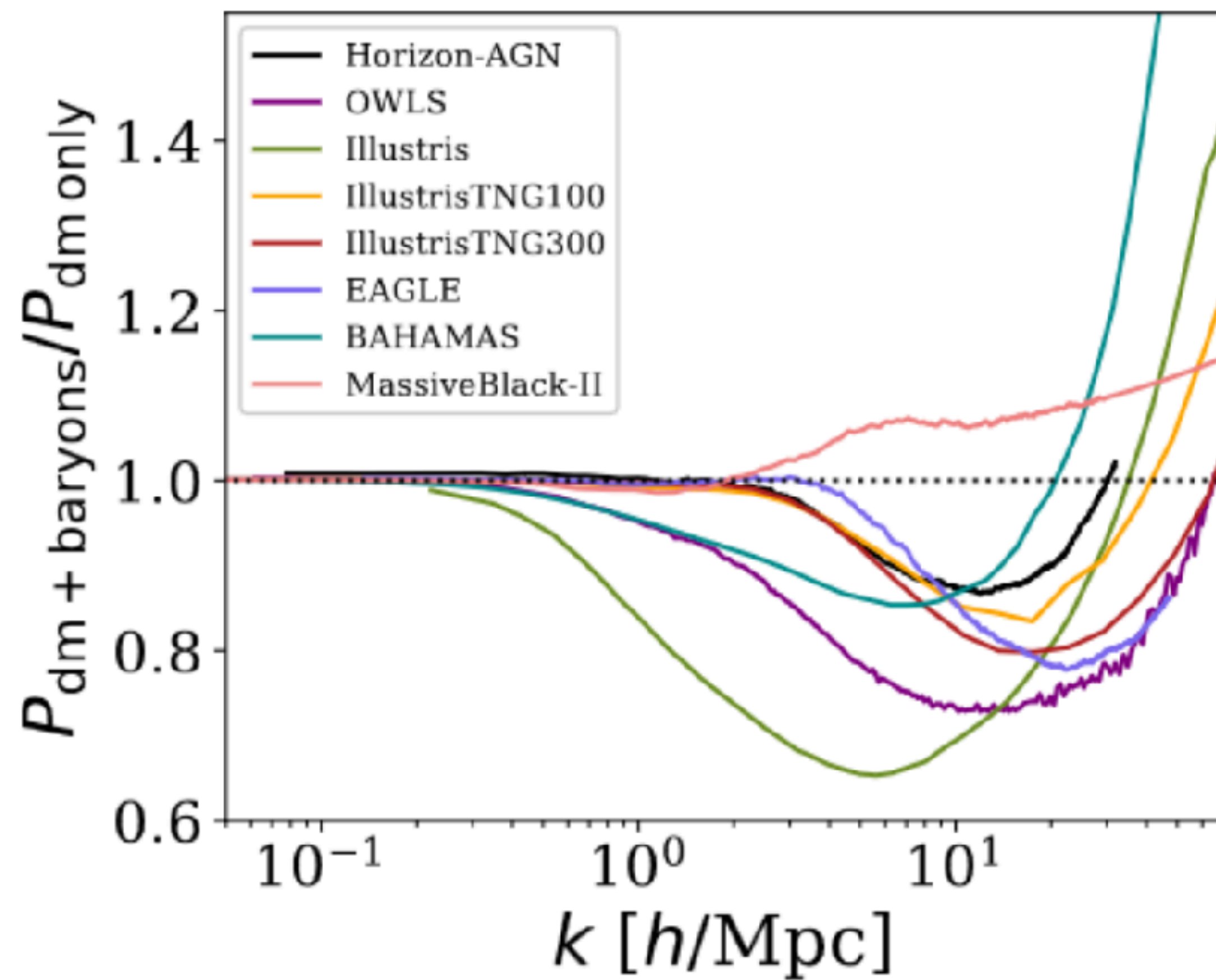
Improvement of ~21%
compared to power spectrum
only.
~35% when combined.

A visualization of the cosmic web, showing a complex network of dark blue filaments and nodes. Numerous bright orange and yellow galaxies are scattered throughout the structure, with a higher concentration at the nodes and along the filaments. The background is a deep, dark blue.

Baryonic feedback

Baryonic feedback

Fractional impact of baryons on the matter power spectrum at $z=0$ for different simulations.

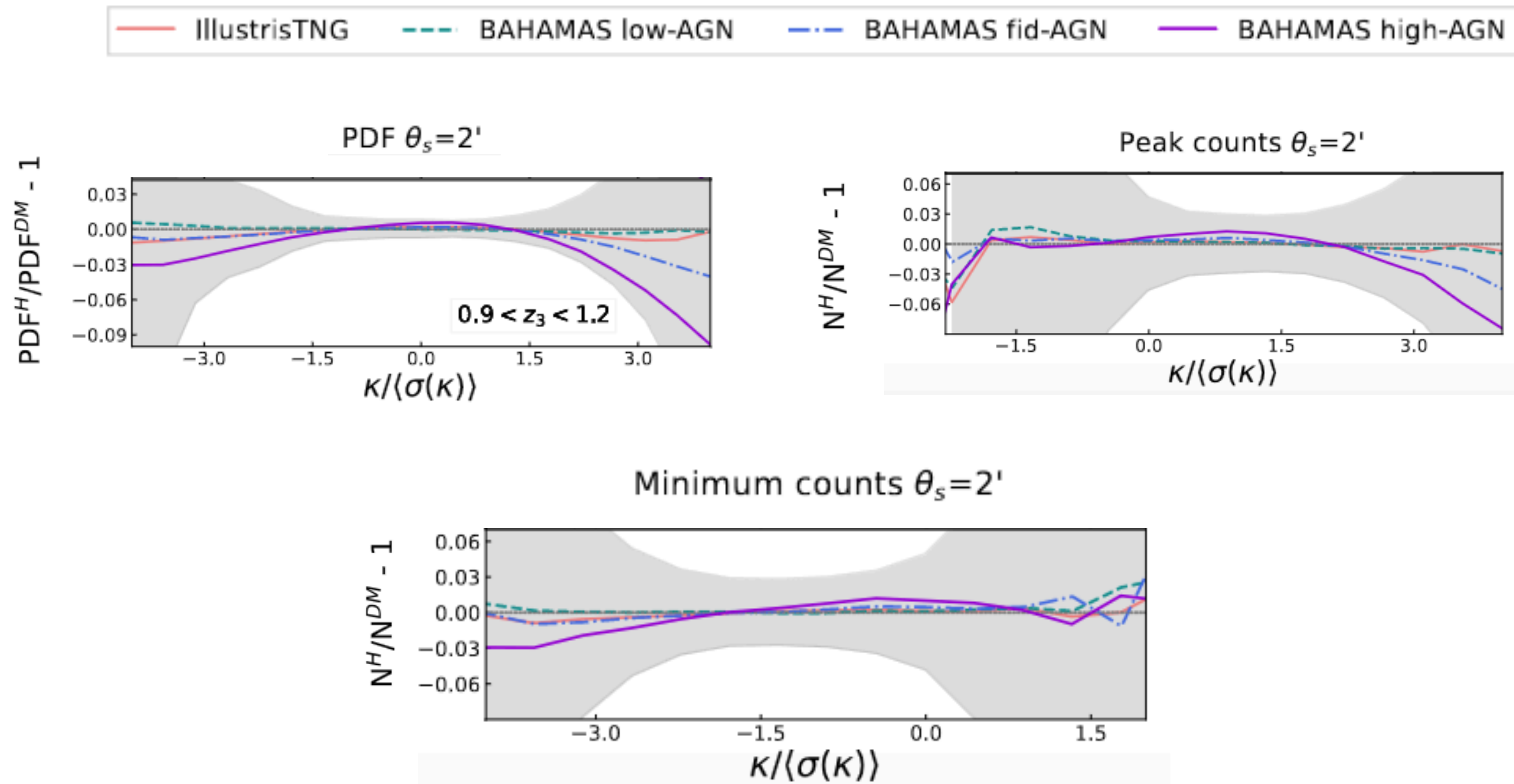


Chisari et al. 2019

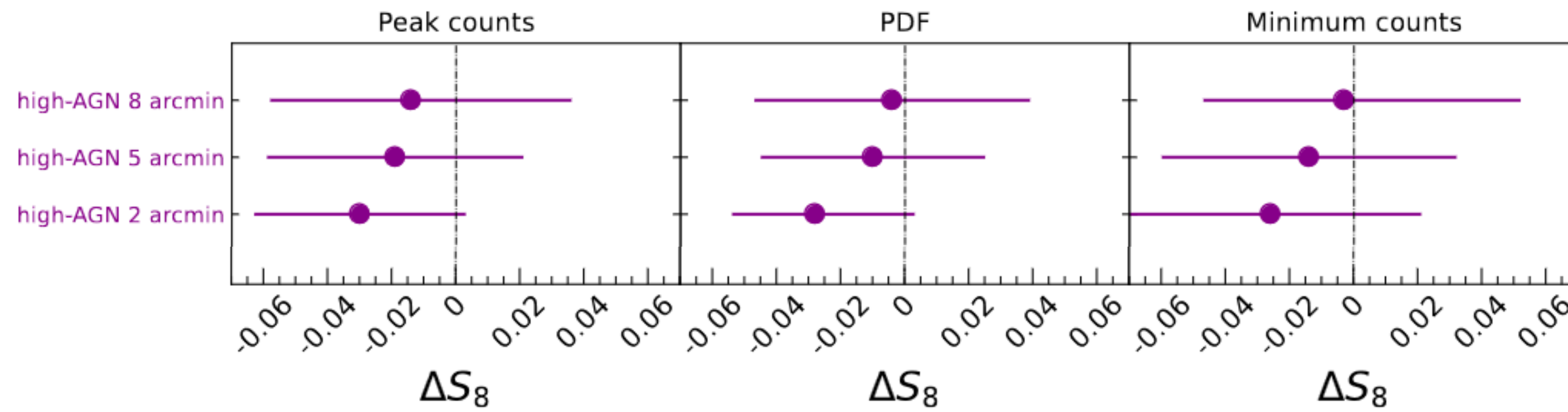
HSC Y1 analysis: Impact of baryons

— IllustrisTNG - - - BAHAMAS low-AGN - · - BAHAMAS fid-AGN — BAHAMAS high-AGN

HSC Y1 analysis: Impact of baryons

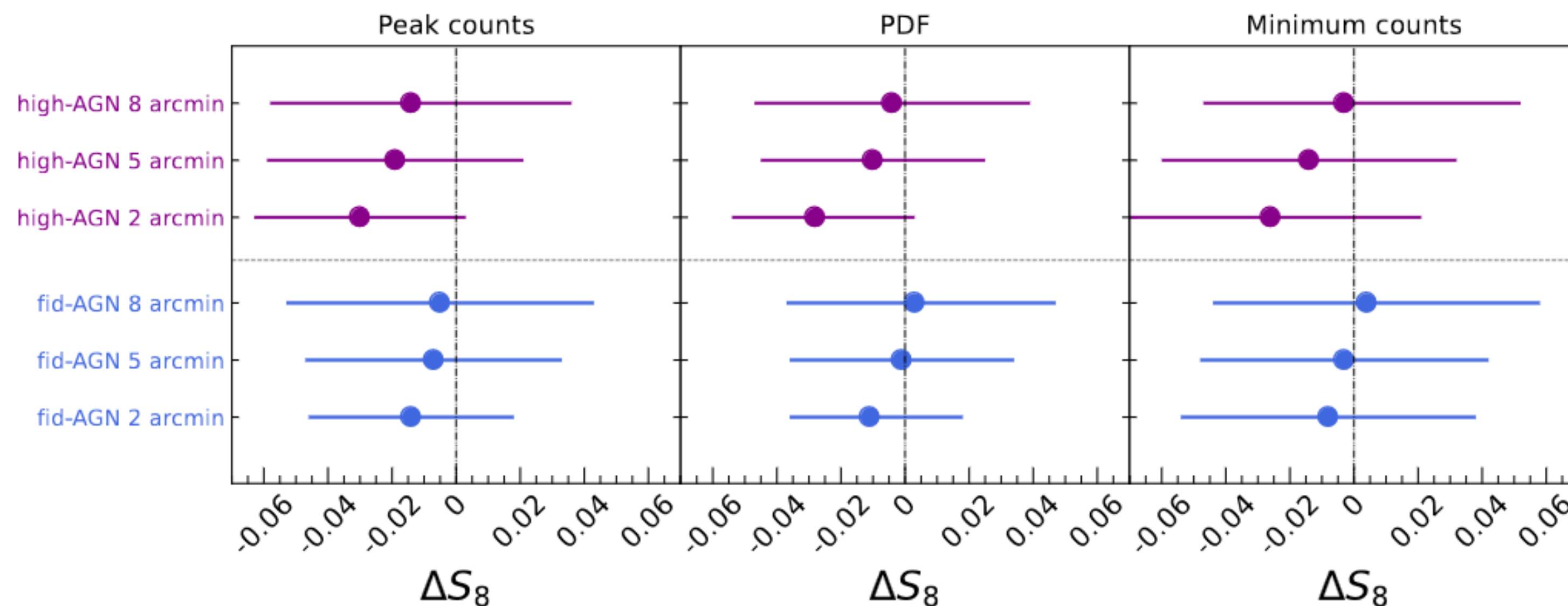


Impact of baryons on the inferred S_8



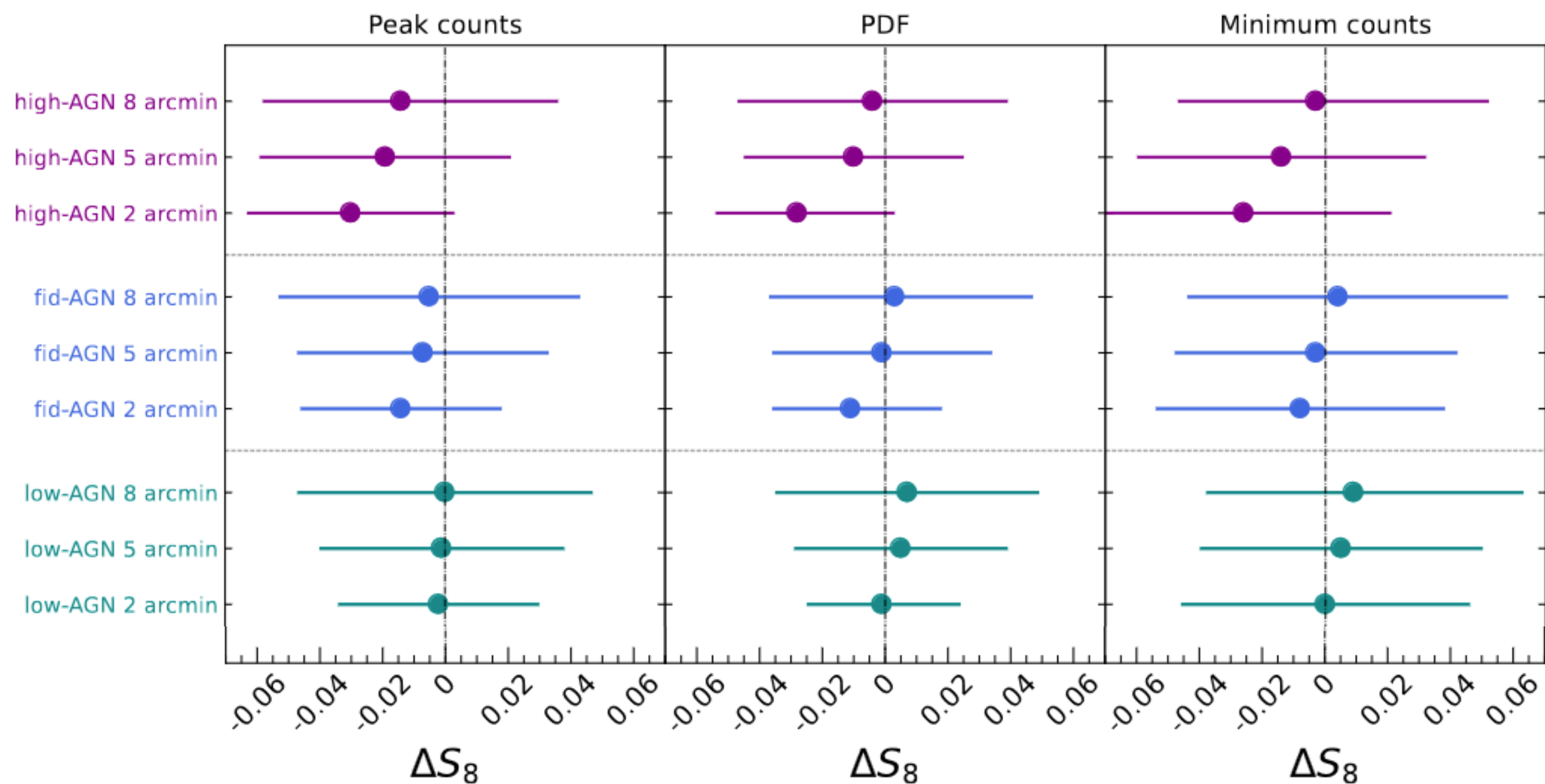
$$\Delta S_8 = S_8^{\text{H}} - S_8^{\text{DM}}$$

Impact of baryons on the inferred S_8



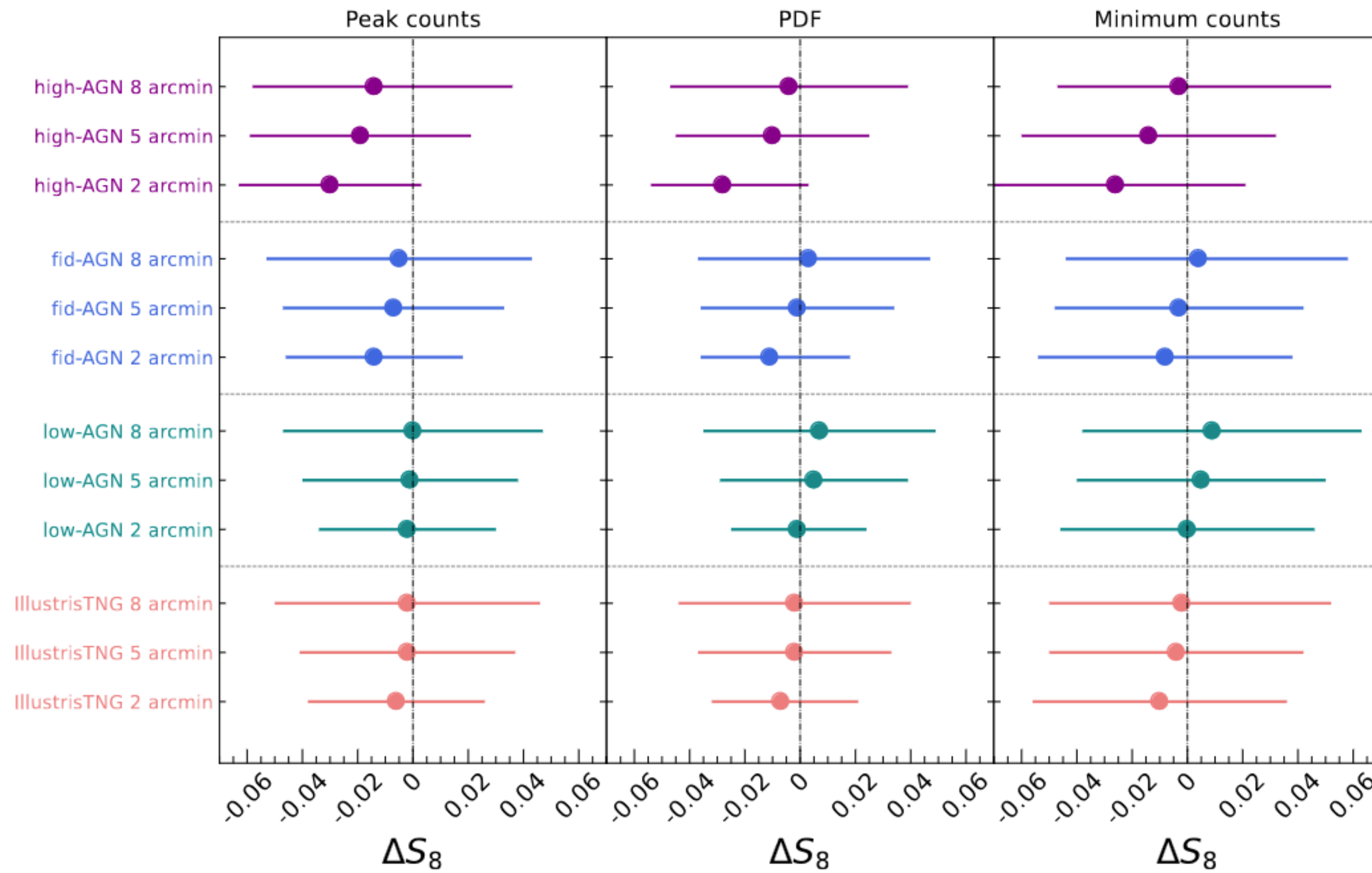
$$\Delta S_8 = S_8^{\text{H}} - S_8^{\text{DM}}$$

Impact of baryons on the inferred S_8



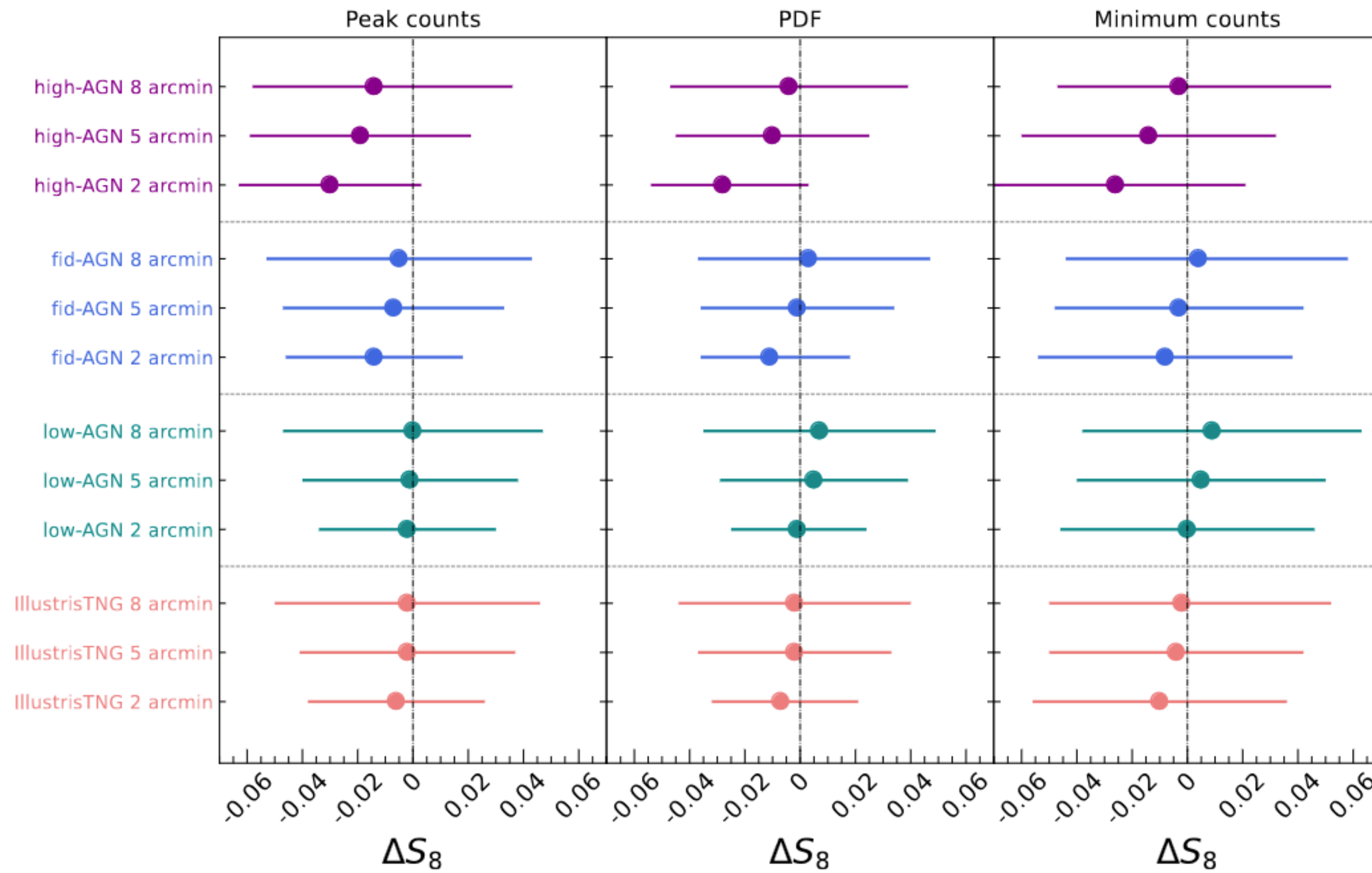
$$\Delta S_8 = S_8^{\text{H}} - S_8^{\text{DM}}$$

Impact of baryons on the inferred S_8



$$\Delta S_8 = S_8^{\text{H}} - S_8^{\text{DM}}$$

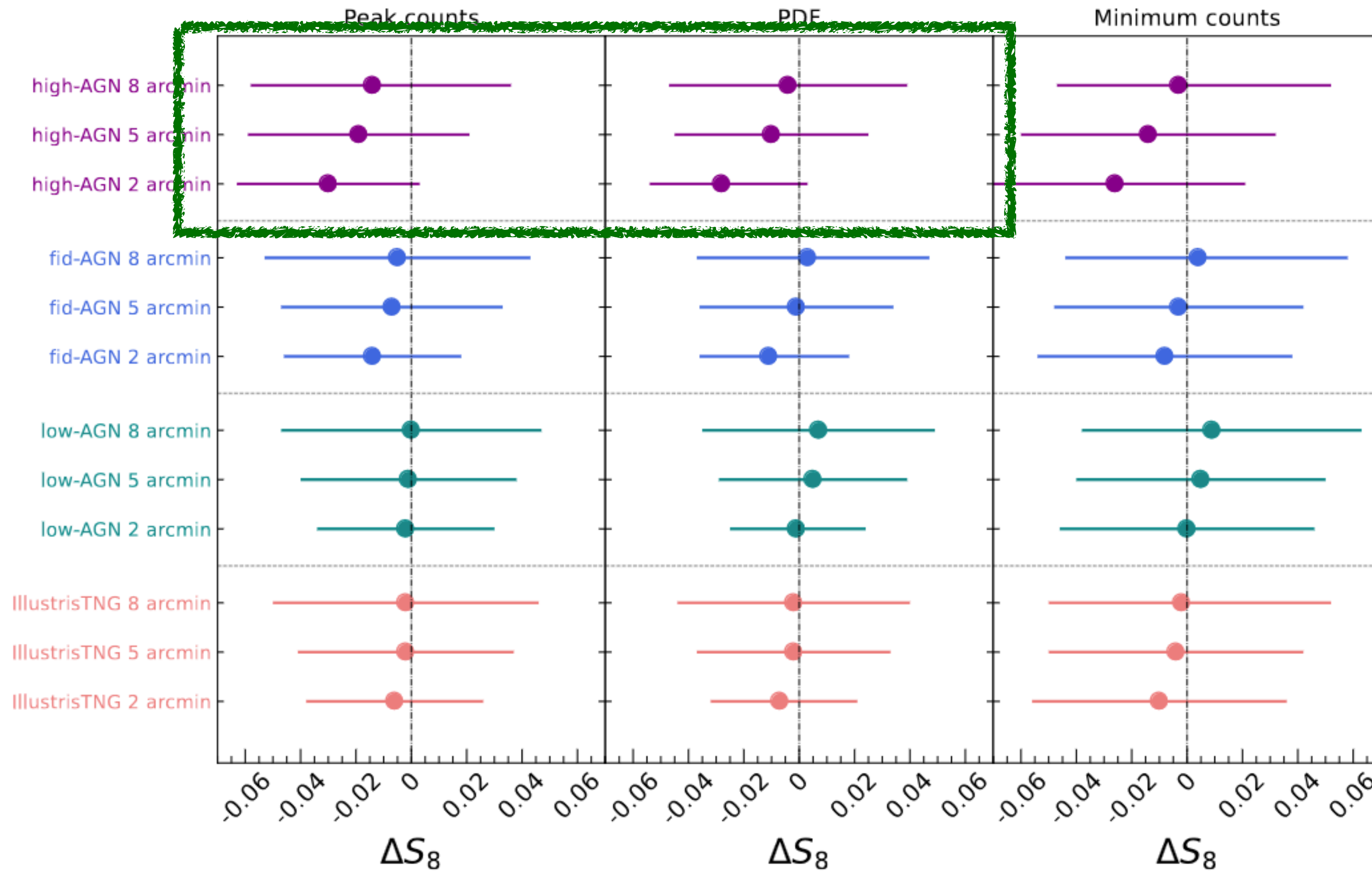
Impact of baryons on the inferred S_8



$$\Delta S_8 = S_8^{\text{H}} - S_8^{\text{DM}}$$

$<1\sigma$ bias in S_8 .

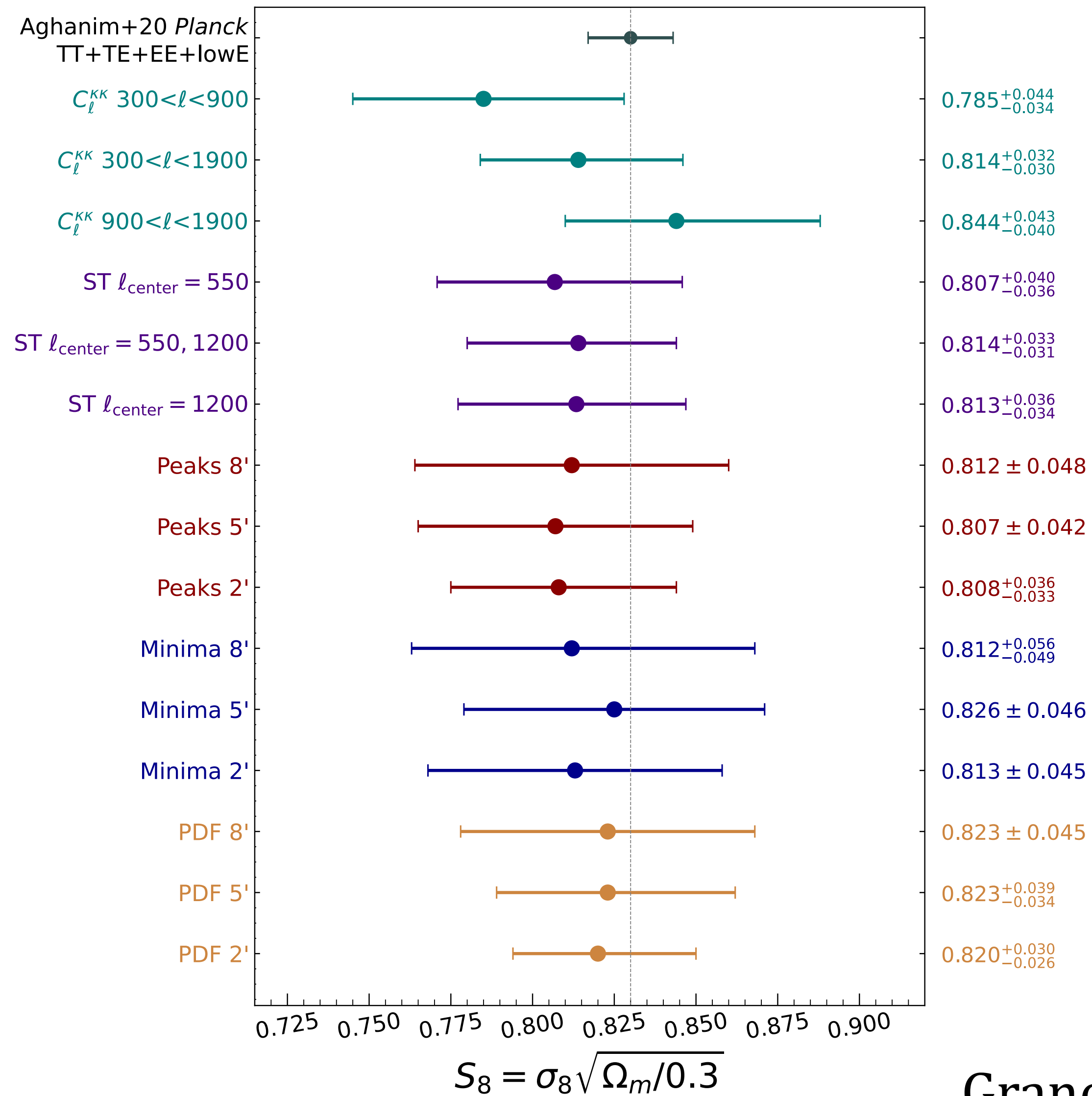
Impact of baryons on the inferred S_8



$$\Delta S_8 = S_8^{\text{H}} - S_8^{\text{DM}}$$

$<1\sigma$ bias in S_8 .

Results: HSC Y1 real data

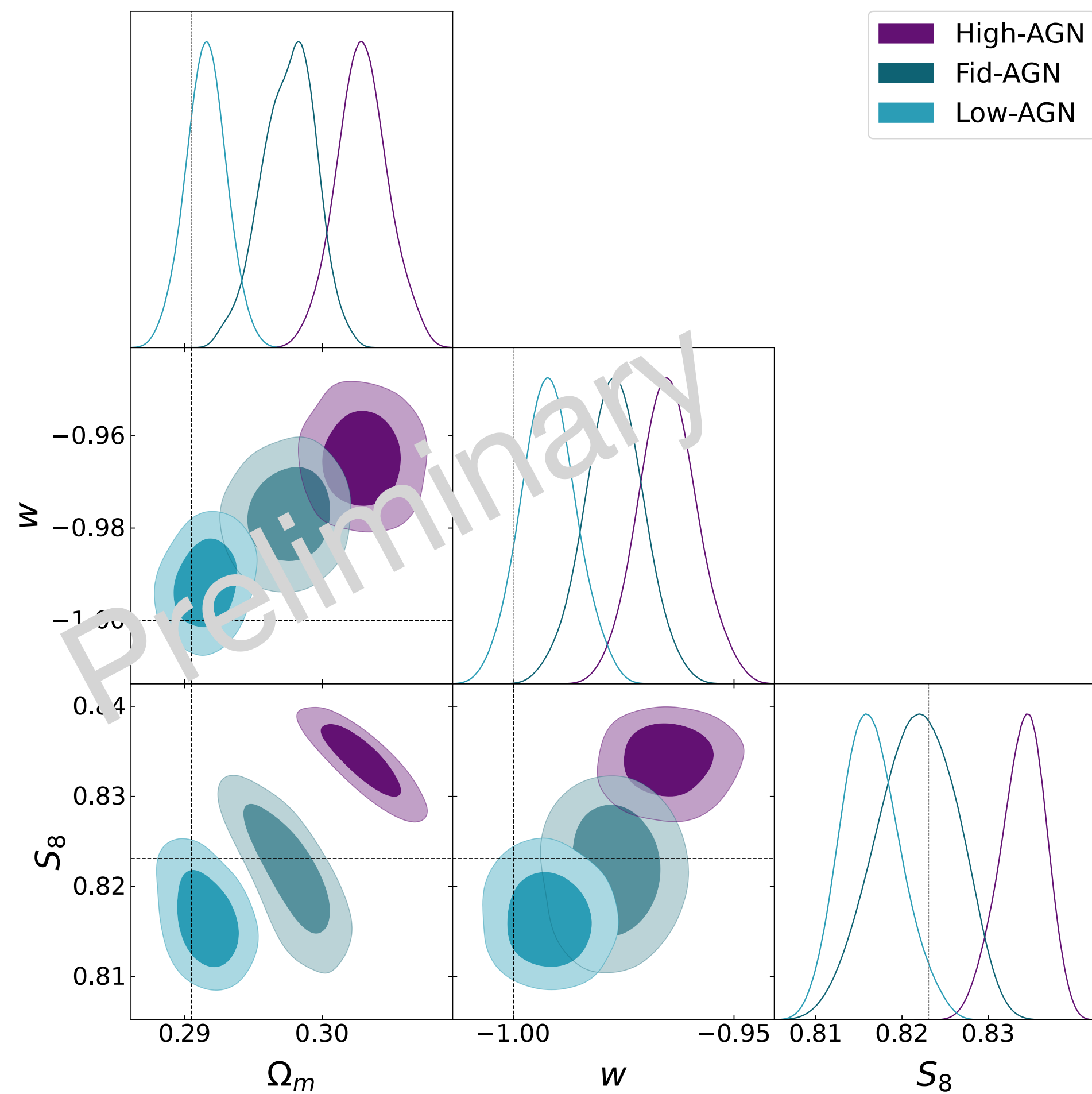


A visualization of the cosmic web, showing a complex network of dark blue filaments and nodes. Numerous bright orange and yellow galaxies are scattered throughout the structure, with a higher concentration at the nodes and along the filaments. The background is a deep, dark blue.

Baryonic feedback and Stage IV analysis

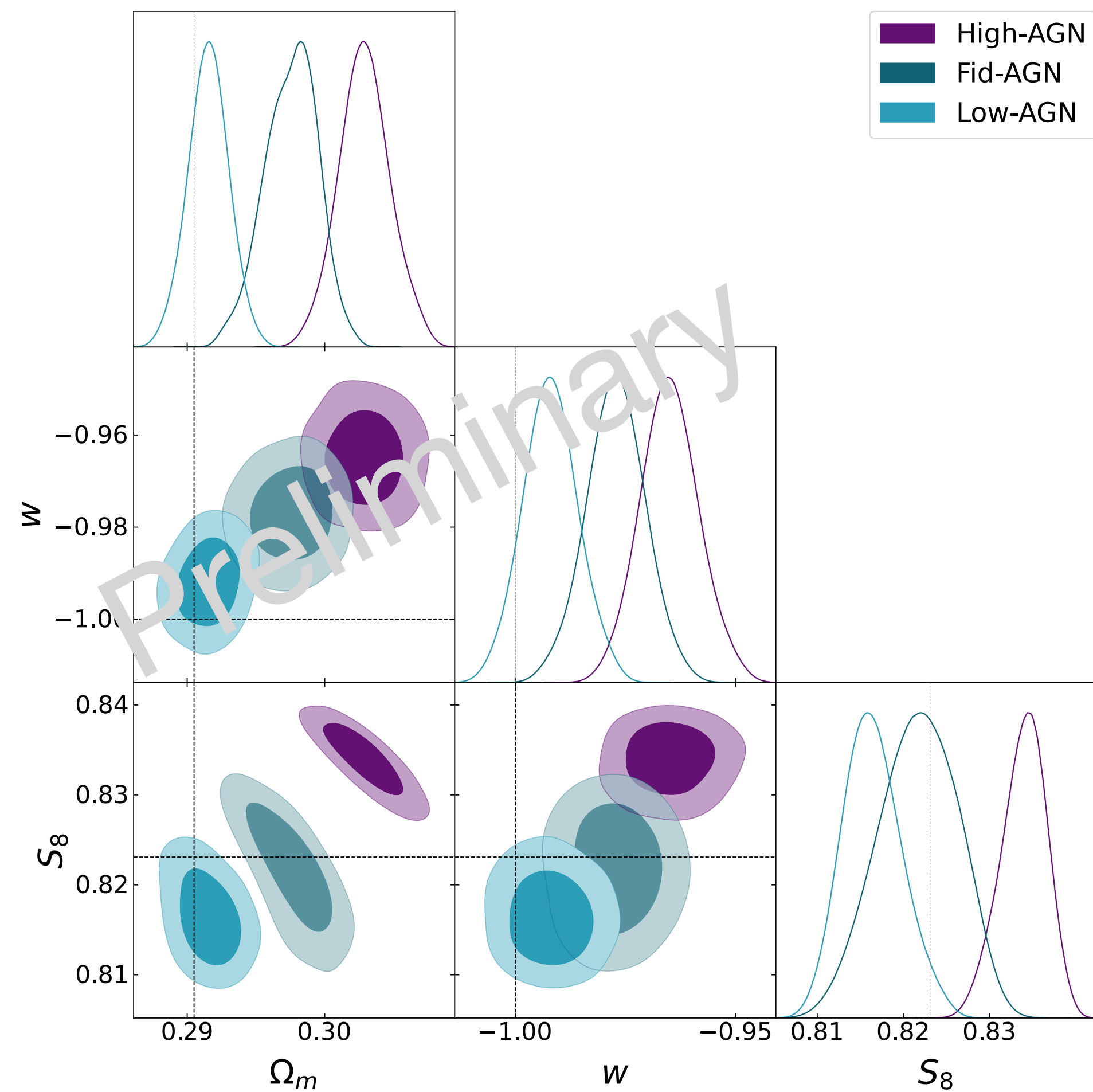
Impact of baryons for Stage IV: Peak counts

Peak counts 2 arcmin

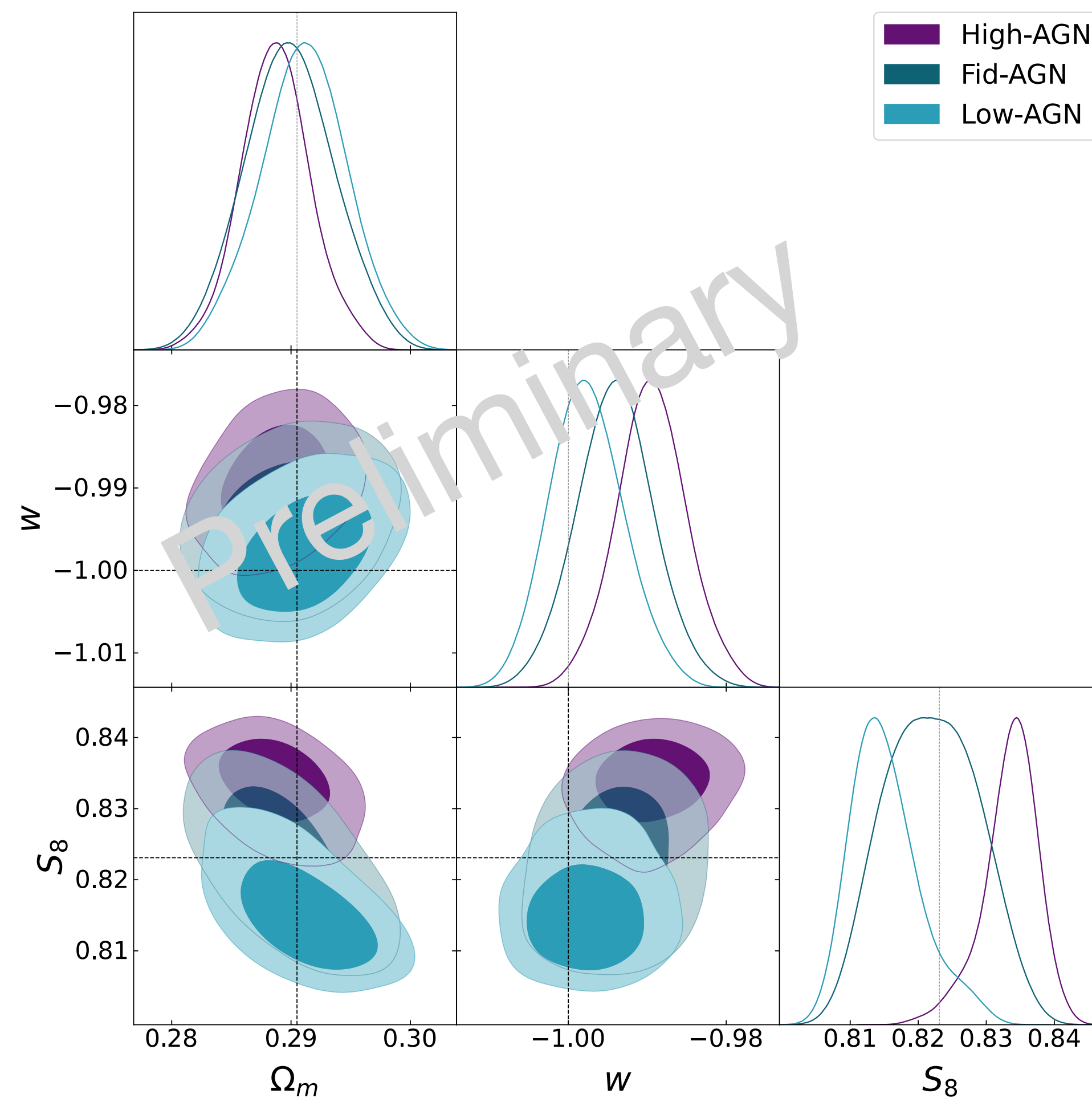


Impact of baryons for Stage IV: Peak counts

Peak counts 2 arcmin



Peak counts 5 arcmin



Baryons and Stage-IV surveys: Bayesian Model Averaging

Our goal is to establish a Bayesian framework that enables trustworthy parameter inference from non-Gaussian statistics, applied to real data.

Bayesian Model Averaging (BMA)

Weighted average of multiple models (baryonic feedback models). Weights determined by the Bayesian evidence.

$$\mathcal{P}(\boldsymbol{\theta}|\boldsymbol{x}) = \frac{\sum_k \mathcal{P}(\boldsymbol{\theta}|\boldsymbol{x}, M_k) \mathcal{P}(M_k|\boldsymbol{x})}{\sum_k \mathcal{P}(M_k|\boldsymbol{x})}$$

The models M_k : BAHAMAS low-AGN, fid-AGN, high-AGN.

Baryons and Stage-IV surveys: Bayesian Model Averaging

Bayesian Model Averaging for Baryonic feedback.

First step: Parameter inference for each model individually.

Likelihood (Sellentin & Heavens 2016):

$$P(\mathbf{x}_o | \boldsymbol{\mu}_B, \mathbf{C}, N_r) = \frac{\bar{c}_p |\mathbf{C}|^{-1/2}}{\left[1 + \frac{(\mathbf{x}_o - \boldsymbol{\mu}_B)^T \mathbf{C}^{-1} (\mathbf{x}_o - \boldsymbol{\mu}_B)}{N_r - 1} \right]^{\frac{N_r}{2}}}$$

Baryons and Stage-IV surveys: Bayesian Model Averaging

Bayesian Model Averaging for Baryonic feedback.

First step: Parameter inference for each model individually.

Likelihood (Sellentin & Heavens 2016):

$$P(\mathbf{x}_o | \boldsymbol{\mu}_B, \mathbf{C}, N_r) = \frac{\bar{c}_p |\mathbf{C}|^{-1/2}}{\left[1 + \frac{(\mathbf{x}_o - \boldsymbol{\mu}_B)^T \mathbf{C}^{-1} (\mathbf{x}_o - \boldsymbol{\mu}_B)}{N_r - 1} \right]^{\frac{N_r}{2}}}$$

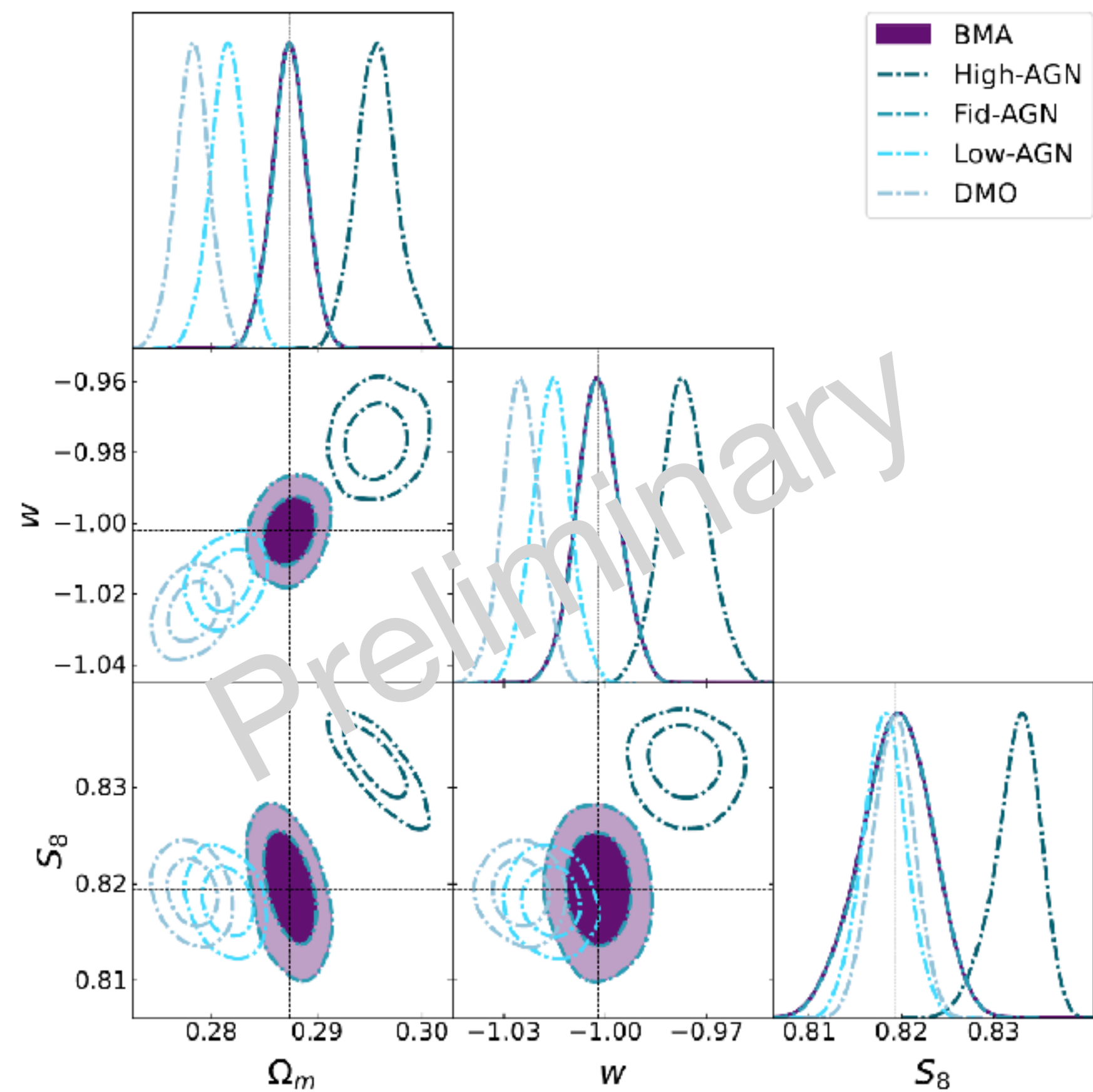
Baryonic feedback correction factor

$$B_i = \frac{\langle x_i^B \rangle}{\langle x_i^{\text{DMO}} \rangle}$$

$$\rightarrow \mu_i^B = \mu_i(\boldsymbol{\theta}) B_i$$

Baryons and Stage-IV surveys: Bayesian Model Averaging

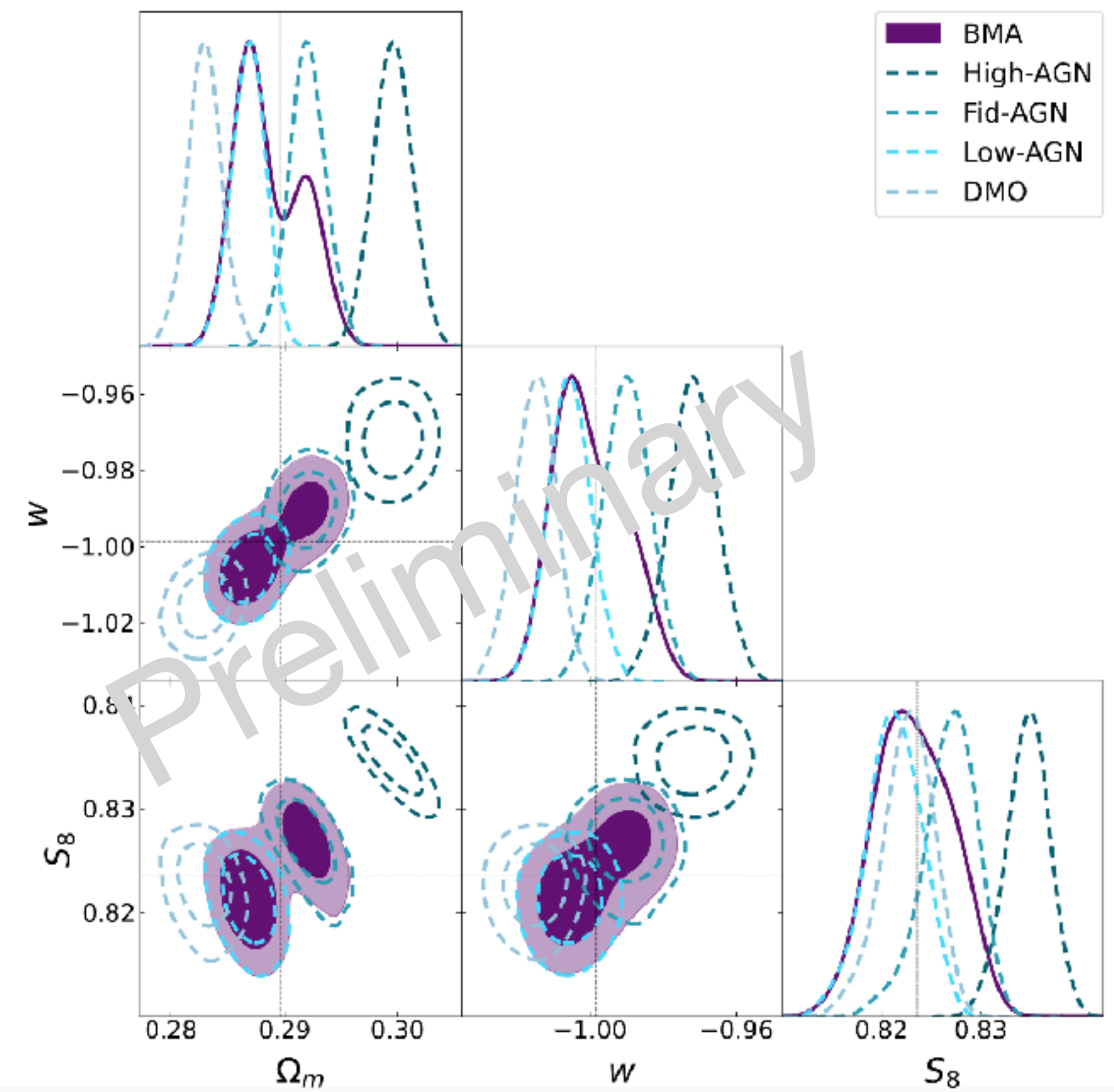
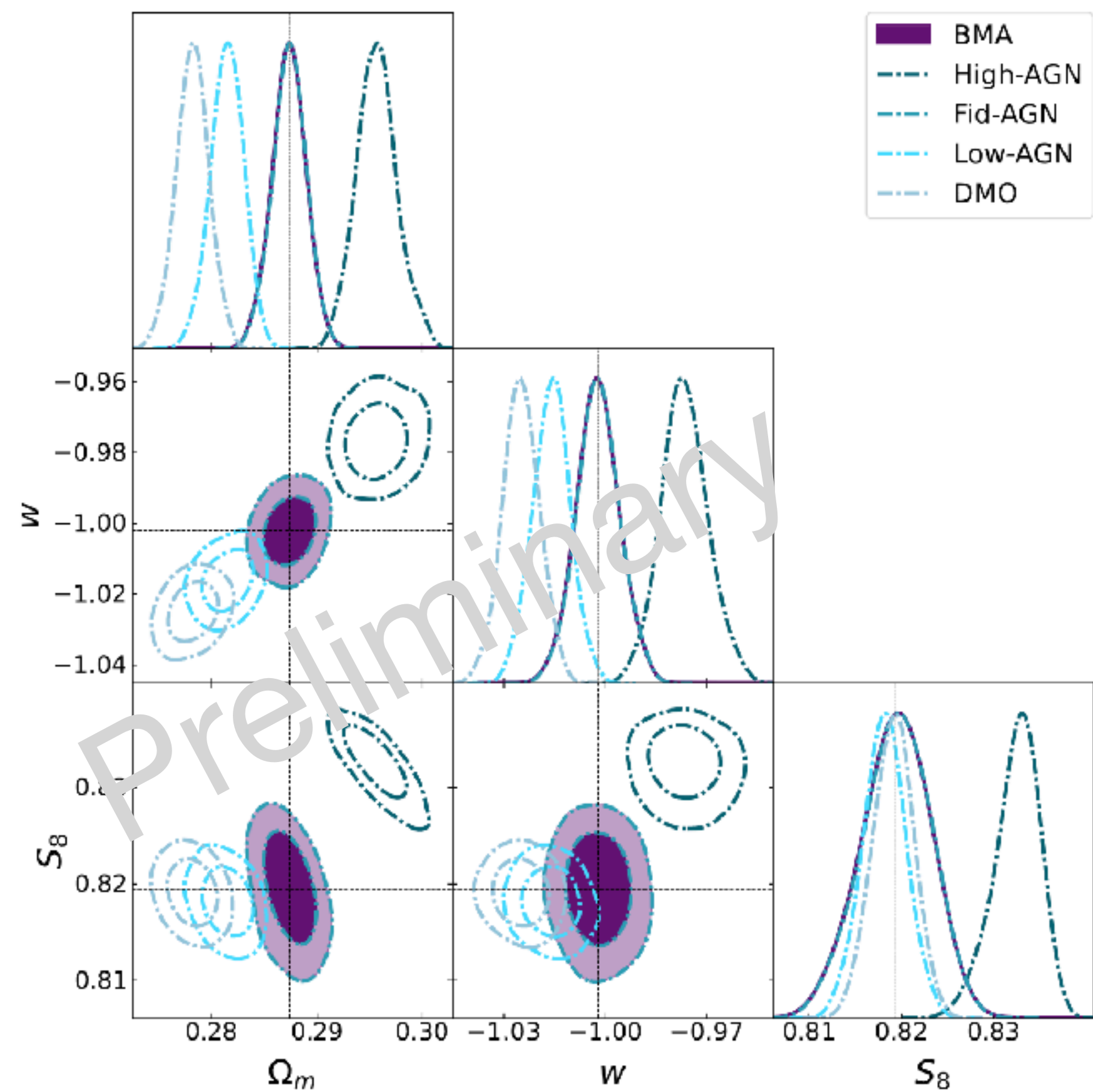
Case 1: Data vector with Fid-AGN contamination



Baryons and Stage-IV surveys: Bayesian Model Averaging

Case 1: Data vector with Fid-AGN contamination

Case 2: Data vector with model misspecification



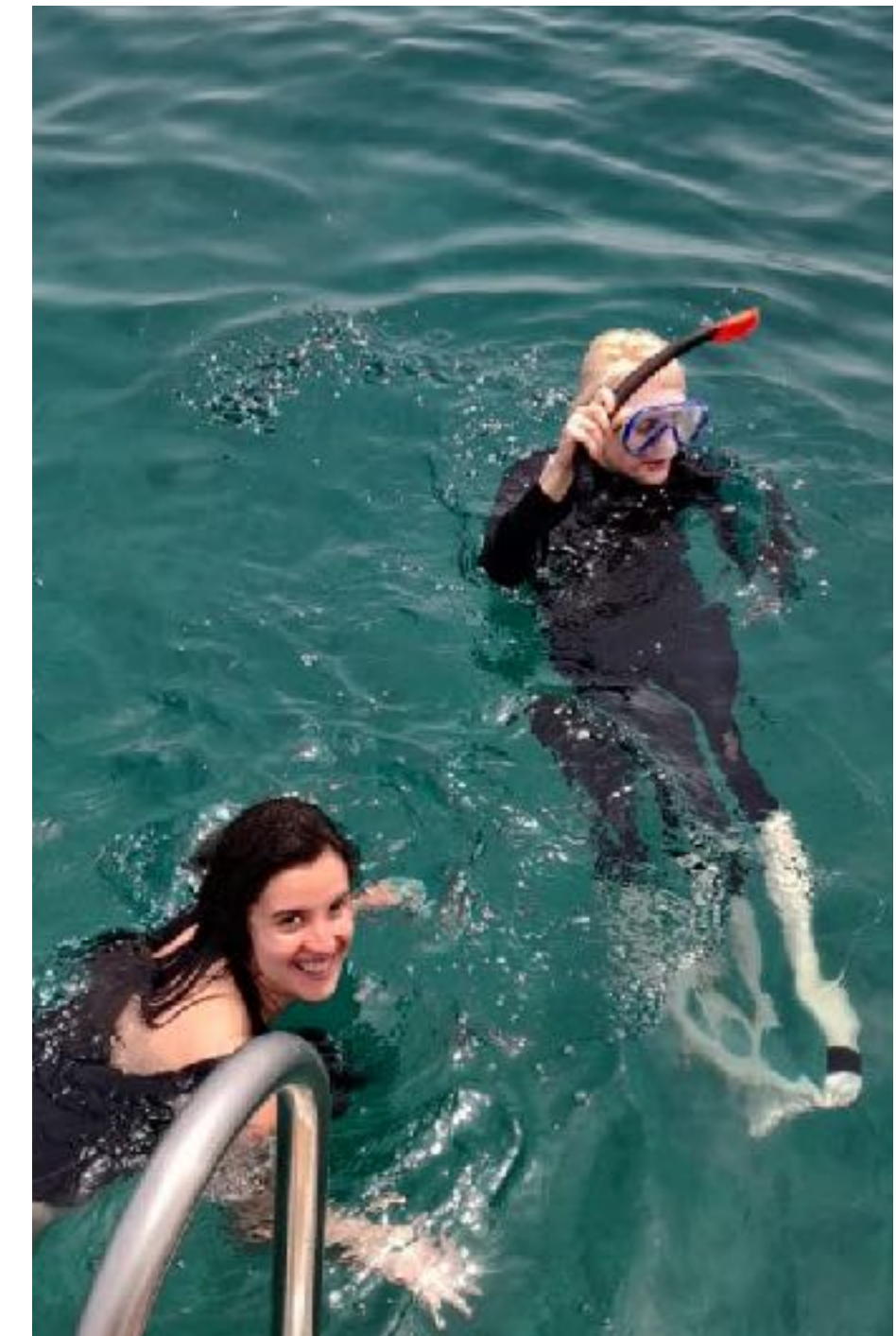
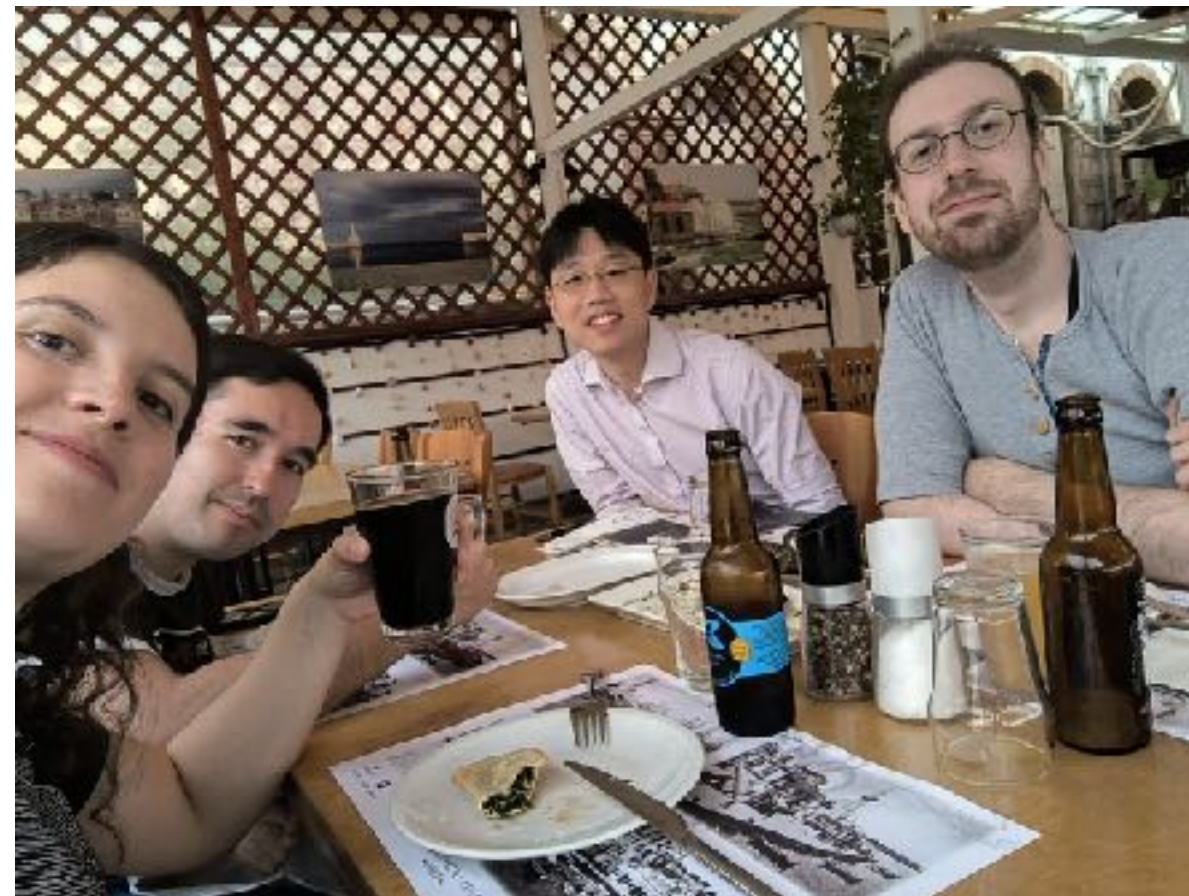
Summary

Non-Gaussian statistics can provide precise cosmological constraints for Stage-III and Stage-IV surveys.

We expect severe biases in cosmological parameters for weak lensing Stage-IV analysis. For peak counts, we need to smooth the map $\ggg 5\text{arcmin}$ in order to debias parameter inference.

Fitting a multitude of baryon models to the data, and having the data select the best model, is a solid technique to inference from non-Gaussian estimators.

Thank you!



Stage III analysis:

Cosmology from weak lensing non-Gaussian stats with Subaru
Hyper Suprime-Cam Y1

Marques et al. 2023 arXiv:2308.10866

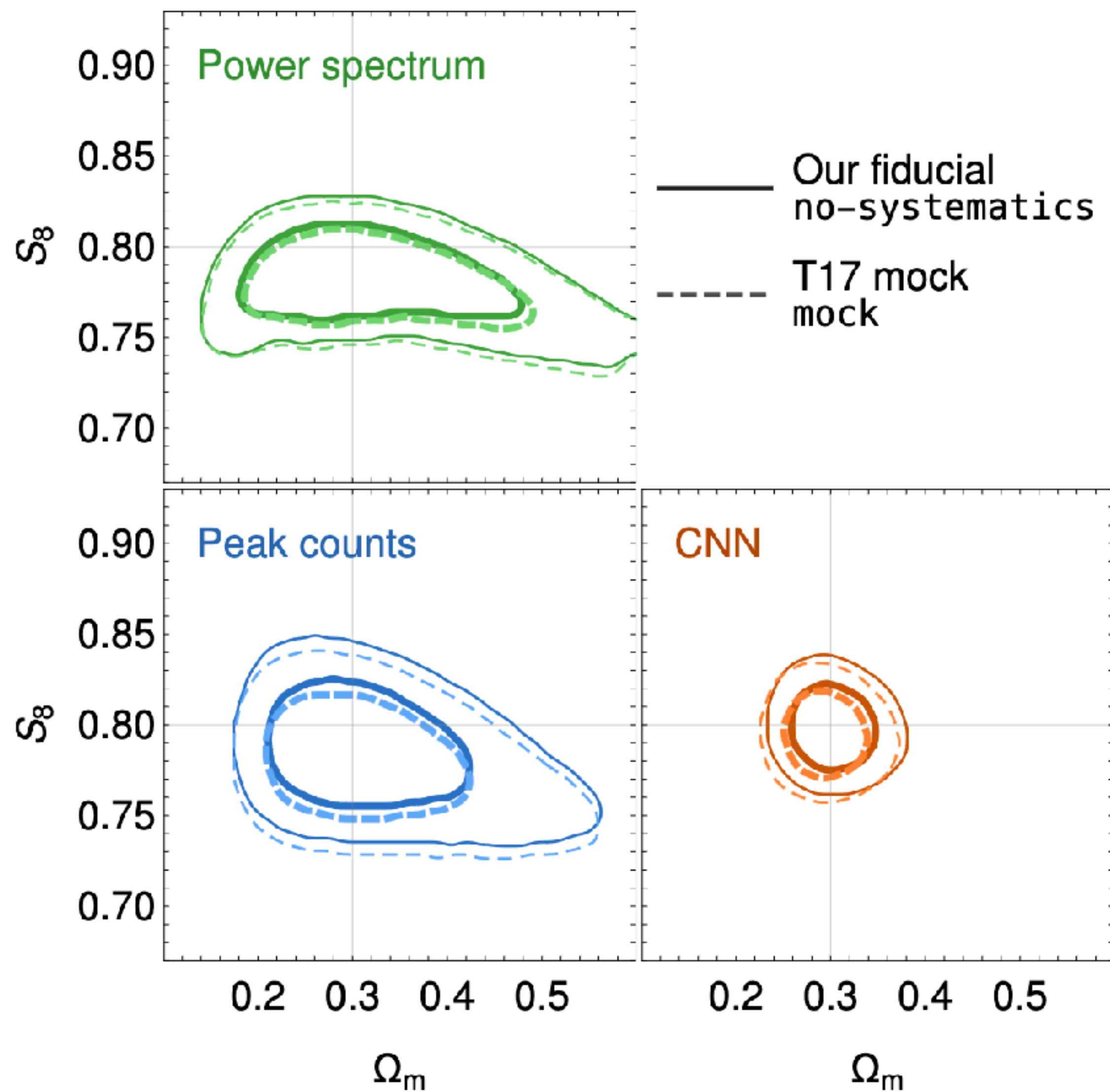
Grandón et al. 2024 arXiv:2403.03807

Thiele et al. 2023 arXiv:2304.05928

Cheng et al. 2024 arXiv:2404.16085



HSC Y1 CNN, Lu et al. 2023



HSC Y1 ST, Cheng et al. 2023

